ESC European Society of Cardiology

Cardiovascular Research (2022) **118**, 2367–2384
https://doi.org/10.1093/cvr/cvab263

Vascular endothelial tissue factor contributes to trimethylamine N-oxide-enhanced arterial thrombosis

Marco Witkowski[1,2], Mario Witkowski[3], Julian Friebel[2,4], Jennifer A. Buffa[1], Xinmin S. Li [1], Zeneng Wang [1], Naseer Sangwan[1], Lin Li [1], Joseph A. DiDonato[1], Caroline Tizian[3], Arash Haghikia [2], Daniel Kirchhofer [5], François Mach [6], Lorenz Räber[7], Christian M. Matter[8,9], W.H. Wilson Tang [1,10], Ulf Landmesser [2,4], Thomas F. Lüscher[8,11], Ursula Rauch[2]*, and Stanley L. Hazen [1,10]*

[1]Department of Cardiovascular & Metabolic Sciences, Lerner Research Institute, 9500 Euclid Ave, Cleveland, OH 44195, USA; [2]Department of Cardiology, Charité Centrum 11, Charité–Universitätsmedizin, Hindenburgdamm 30, 12203, Berlin, Germany; [3]Department of Microbiology, Infectious Diseases and Immunology, Laboratory of Innate Immunity, Charité-Universitätsmedizin Berlin, Berlin, Germany; [4]Berlin Institute of Health, Anna-Louisa-Karsch-Straße 2, 10178, Berlin, Germany; [5]Department of Early Discovery Biochemistry, Genentech, Inc., 1 DNA Way, South San Francisco, CA 94080, USA; [6]Department of Cardiology, University Hospital Geneva, Rue Gabrielle-Perret-Gentil 4 1205, Geneva, Switzerland; [7]Department of Cardiology, Inselspital Bern, Freiburgstrasse 18 CH-3010, Bern, Switzerland; [8]Center for Molecular Cardiology, University of Zurich, Wagistrasse 12, CH-8952 Schlieren, Switzerland; [9]Department of Cardiology, University Heart Center, University Hospital Zurich, Raemistrasse 100 8091, Zurich, Switzerland; [10]Department of Cardiovascular Medicine, Heart, Vascular & Thoracic Institute, Cleveland Clinic, 9500 Euclid Ave, Cleveland, OH, USA; [11]Department of Cardiology, Royal Brompton and Harefield Hospitals, Imperial College, Sydney St, London SW3 6NP, UK

Received 3 March 2021; editorial decision 25 July 2021; accepted 2 August 2021; online publish-ahead-of-print 5 August 2021

Time for primary review: 32 days

Aims

Gut microbiota and their generated metabolites impact the host vascular phenotype. The metaorganismal metabolite trimethylamine N-oxide (TMAO) is both associated with adverse clinical thromboembolic events, and enhances platelet responsiveness in subjects. The impact of TMAO on vascular Tissue Factor (TF) *in vivo* is unknown. Here, we explore whether TMAO-enhanced thrombosis potential extends beyond TMAO effects on platelets, and is linked to TF. We also further explore the links between gut microbiota and vascular endothelial TF expression *in vivo*.

Methods and results

In initial exploratory clinical studies, we observed that among sequential stable subjects ($n = 2989$) on anti-platelet therapy undergoing elective diagnostic cardiovascular evaluation at a single-site referral centre, TMAO levels were associated with an increased incident (3 years) risk for major adverse cardiovascular events (MACE) (myocardial infarction, stroke, or death) [4th quartile (Q4) vs. Q1 adjusted hazard ratio (HR) 95% confidence interval (95% CI), 1.73 (1.25–2.38)]. Similar results were observed within subjects on aspirin mono-therapy during follow-up [adjusted HR (95% CI) 1.75 (1.25–2.44), $n = 2793$]. Leveraging access to a second higher risk cohort with previously reported TMAO data and monitoring of anti-platelet medication use, we also observed a strong association between TMAO and incident (1 year) MACE risk in the multi-site Swiss Acute Coronary Syndromes Cohort, focusing on the subset ($n = 1469$) on chronic dual anti-platelet therapy during follow-up [adjusted HR (95% CI) 1.70 (1.08–2.69)]. These collective clinical data suggest that the thrombosis-associated effects of TMAO may be mediated by cells/factors that are not inhibited by anti-platelet therapy. To test this, we first observed in human microvascular endothelial cells that TMAO dose-dependently induced expression of TF and vascular cell adhesion molecule (VCAM)1. In mouse studies, we observed that TMAO-enhanced aortic *TF and VCAM1* mRNA and protein expression, which upon immunolocalization studies, was shown to co-localize with vascular endothelial cells. Finally, in arterial injury mouse models, TMAO-dependent enhancement of *in vivo* TF expression and thrombogenicity were abrogated by either a TF-inhibitory antibody or a mechanism-based microbial choline TMA-lyase inhibitor (fluoromethylcholine).

Conclusion

Endothelial TF contributes to TMAO-related arterial thrombosis potential, and can be specifically blocked by targeted non-lethal inhibition of gut microbial choline TMA-lyase.

* Corresponding author. Tel: +1 216 445 9763; fax: +1 216 444 9404, E-mail: hazens@ccf.org (S.L.H.); Tel: +49 30 8445 2362; fax: +49 30 8445 4648, E-mail: ursula.rauch@charite.de (U.R.)

Graphical Abstract

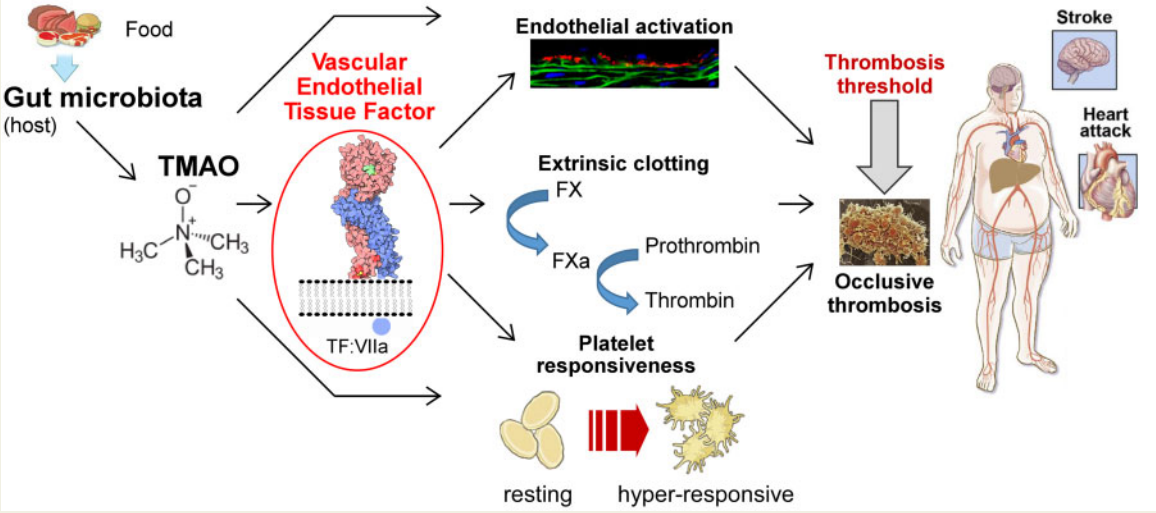

Keywords Microbiome • Trimethylamine N-oxide • Cardiovascular disease • Thrombosis • Tissue factor

1. Introduction

The microbiome is critically involved in the vascular complications of cardiovascular disease (CVD).[1–5] Gut microbiota both contribute to cardiovascular homeostasis and shape the vascular phenotype through generation of metaorganismal (involving both microbe and host) metabolites that either directly or indirectly impact host physiology.[5–10] However, our mechanistic understanding of how gut microbes affect thrombotic complications of atherosclerosis, the hallmark of acute coronary syndromes (ACS) and the primary cause of death in CVD, remains incomplete. The microbiota-dependent metabolite trimethylamine N-oxide (TMAO) has been both clinically and mechanistically linked to CVD[7,11–21] and thrombotic complications.[19,22–24] TMAO synthesis begins with dietary precursors that are abundant in various foods (e.g. red meat, which contains high levels of the precursors choline and carnitine), which are then metabolized by gut microbiota TMA-lyases to form trimethylamine (TMA).[5,24–26] Following absorption into the portal circulation, TMA is rapidly oxidized in the host liver by flavin monooxygenases, thereby forming TMAO.[7,27] Meta-analyses of multiple clinical studies confirm circulating TMAO levels are strongly associated with incident major adverse cardiovascular events (MACE) (myocardial infarction, stroke, and death) and adverse cardiovascular outcomes in subjects, including amongst subjects with heart failure.[28–31] A common theme observed in cases of elevated TMAO is its association with vascular phenotypes linked to a 'vulnerable plaque', including effects on both the vessel wall and circulating cells.[22,32–35] Further, mechanistic studies in both animals and humans have revealed that TMAO potentiates platelet calcium signalling, platelet aggregation to multiple agonists, vascular inflammation, and *in vivo* thrombosis.[5,19,22,24,36–40] Despite these findings, it is unclear whether TMAO-dependent enhancement of *in vivo* thrombosis extends beyond platelets and involves TMAO-associated alterations of coagulation factors. Moreover, it remains unknown whether the striking clinical association between TMAO and adverse thrombotic event risk can be observed in the presence of anti-platelet drugs, such as aspirin, adenosine diphosphate (ADP)-receptor antagonists, or their combination [dual anti-platelet therapy (DAPT)].

Tissue Factor (TF) is the membrane-bound receptor for Factor(F)VII/VIIa, and the primary initiator of the extrinsic pathway of blood coagulation.[41–43] TF is constitutively expressed in the perivascular space and triggers activation of FIX to FIXa and FX to FXa, leading to thrombin generation. TF thus plays an essential role in haemostasis following vascular injury.[41–43] During atherosclerotic CVD and vascular inflammation, enhanced expression of both full length (fl) TF and its soluble alternatively-spliced isoform (asTF) are observed within the vessel wall and blood cells, contributing to a pro-thrombotic state and vascular complications.[44–49] In particular, it is widely accepted that vessel wall-derived TF critically contributes to *in vivo* thrombosis initiation, through mechanisms involving local thrombin generation, which induces platelet activation and release of secondary platelet agonists, such as ADP, at the site of injury.[50,51] Thus, processes that lead to heightened vascular TF expression are of interest.

Despite the numerous clinical and mechanistic links between the metaorganismal TMAO pathway and enhanced clotting risks (both in clinical studies and in animal models of thrombosis), a role for TF in contributing to TMAO-dependent enhanced thrombosis *in vivo* remains to be established. Herein, we first examined in two distinct clinical studies whether TMAO-related thrombotic risk extends to patients who are on anti-platelet drugs, including aspirin with or without ADP-receptor antagonists. Then, through various mechanistic and animal models of arterial injury and thrombosis, we explored whether TMAO induces endothelial TF and VCAM1 expression, and whether TMAO-stimulated TF expression contributes to TMAO-enhanced thrombosis potential *in vivo*.

Finally, we both tested whether selective non-lethal pharmacological targeting of gut microbe-dependent TMAO generation attenuates choline diet-induced TF expression and heightened thrombogenicity, and identified caecal microbial taxa whose proportions are associated with TMAO-enhanced TF pathway activation and thrombosis.

2. Material and methods

2.1 Ethical statement

All enrolled participants in the Cleveland Clinic Genebank study gave written informed consent for a protocol that was approved by the Cleveland Clinic Institutional Review Board.

For the multi-site Swiss Special Program University Medicine Acute Coronary Syndromes (SPUM-ACS) cohort all subjects gave written informed consent, and the study was approved by the institutional review board (Ethics Committee of the Canton of Zurich, Switzerland). Both studies were in accordance with the principles outlined in the Declaration of Helsinki. All animal model studies were approved by the Institutional Animal Care and Use Committee at the Cleveland Clinic (Protocol # 2018-2082).

2.2 Human studies

For clinical studies, we leveraged access to data from two independent study cohorts with already reported TMAO data[7,52] to explore whether TMAO retained clinical prognostic value in subjects on chronic anti-platelet agent therapy. We thus focused analyses on patients documented to have remained on anti-platelet therapy throughout the duration of follow-up. The Cleveland Clinic Genebank study (clinicaltrials.gov Identifier: NCT00590200) is a large, single-centre, prospective cohort study with cardiovascular outcomes in individuals undergoing elective diagnostic coronary angiography at the Cleveland Clinic from 2001 to 2007. We have previously reported that TMAO levels among Genebank subjects ($n = 4007$) predict CVD risks.[7] In this study, analysis included only the subset of sequential patients that received anti-platelet therapy (aspirin or an ADP-antagonist, $n = 2989$) throughout the follow-up period (3 years). The adjudicated occurrence of MACE was defined as a composite of death, non-fatal myocardial infarction, or non-fatal stroke.

The SPUM-ACS cohort is a prospective multi-site cohort that enrolled patients who underwent coronary angiography for ACS at any of the participating University Hospitals (Zurich, Bern, Lausanne, and Geneva).[52] We have previously reported that in the Swiss ACS Cohort ($n = 1683$) TMAO levels were associated with event risk.[53] As per protocol, upon enrolment in the Swiss ACS Cohort, patients were either placed on aspirin alone (e.g. in case of coronary artery bypass grafting), DAPT (defined as aspirin 100 mg/d plus ADP-receptor antagonist, i.e. either ticagrelor 90 mg twice daily for non-ST-elevation myocardial infarction, or prasugrel 10 mg/d for ST-elevation myocardial infarction), or a combination of oral anticoagulants and anti-platelet agent agents when indicated. The present analysis only included the subset ($n = 1469$) of SWISS ACS Cohort patients that received DAPT throughout the follow-up period. The adjudicated occurrence of MACE (death, non-fatal myocardial infarction, non-fatal stroke or need for revascularization) was recorded during the first year of follow-up.

In both cohorts, circulating levels of TMAO levels in plasma were determined by stable isotope dilution high-performance liquid chromatography with on line electrospray ionization tandem mass spectrometry (LC/MS/MS) using d9-(trimethyl)-labelled internal standard, as described previously.[54]

2.3 Mouse studies and mass spectrometry

Female C57BL/6J mice (Stock No 000664, Jackson Laboratory, Bar Harbor, ME, USA) were bred and maintained on Teklad (Envigo, Indianapolis, IN, USA) diet 2918 (an irradiated global 18% protein rodent diet). For studies involving acute TMAO exposure, the mice were given a single bolus injection intraperitoneally of TMAO or vehicle (normal saline) to achieve physiological levels of circulating TMAO as previously described.[22] Resulting plasma TMAO levels are reported. As a positive control for vascular TF expression and thrombin–anti-thrombin complex (TAT) levels, mice were intraperitoneally injected with 15 mg/kg lipopolysaccharide (LPS) (Catalogue # L2630, Sigma, St. Louis, MO, USA). Blood and tissues were harvested from mice following intraperitoneal injection at the following times: 1.5 h for RNA, 6 h for protein and TAT levels, and at both 1.5 h and 6 h for mass spectrometry analyses.

Chronic TMAO and choline exposures were also examined using dietary supplementation. During breeding and routine housing prior to randomization into dietary arms, animals were put on a control diet (Teklad 2018, Envigo, Indianapolis, IN, USA,), a global 18% protein standard rodent diet without added choline that was documented to contain 0.08 g% of total choline content by mass spectrometry. At indicated time points, animals were randomized to either this control (chow) diet or a choline-supplemented diet (the control diet supplemented with an additional 1 g% choline). Where indicated, mice were also treated with fluoromethylcholine (FMC) in the drinking water (0.006% weight/volume of the salt, which corresponds to ~10 mg/kg/day). Animals were fed *ad libitum* on the indicated diets for at least 10 days before euthanasia and tissue collection. Blood was drawn by vena cava puncture and 10% sodium citrate added. Choline content of food, plasma levels of TMAO, and choline were quantified by stable isotope dilution LC/MS/MS as previously described.[7]

2.4 *In vivo* thrombosis

A common carotid artery $FeCl_3$ induced injury model was performed as previously described.[22] Where indicated, animals were injected with either the neutralizing rat anti-mouse TF antibody 1H1[55] (20 mg/kg), or an isotype-matched control antibody (20 mg/kg of rat IgG2a κ isotype control, clone eBR2a, eBioscience San Diego, CA, USA) 1 h before performing the injury model, as described.[56] Briefly, rhodamine 6G (100 µL; 0.5 mg/mL, catalogue # 252433, Sigma, St. Louis, MO, USA) was injected into the right jugular vein to label platelets. The left carotid artery was then exposed to a Whatman filter paper (Catalogue # 1003-055, GE healthcare, Chicago, IL, USA) of 1 mm^2 size, soaked in 10% $FeCl_3$ (Catalogue # 157740, Sigma, St. Louis, MO, USA) for 1 min. Thrombus formation was observed in real time using intravital fluorescence microscopy and video image capture. Time to complete cessation of blood flow was determined by visual inspection of computer images by two independent investigators blinded to mouse treatment group, and end points with complete thrombotic occlusion were set as cessation of blood flow for more than 30 s. Following the procedure, blood was drawn for plasma isolation, and carotid arteries with thrombi were recovered for immunohistochemical analyses.

All animals (acutely injected with vehicle, TMAO or LPS, on different diets outlined above or used for *in vivo* thrombosis) were euthanized following AVMA guidelines (2020, https://certifiedhumane.org/wp-content/uploads/2020-Euthanasia-Final-1-17-20.pdf) by intraperitoneal injection

of 300 mg/kg ketamine + 30 mg/kg xylazine. Death was assured by post mortem exsanguination and removal of vital organs prior to disposal. For *in vivo* thrombosis animals were anesthetized by administering IP 100 mg/kg ketamine + 10 mg/kg xylazine. Up to 50 mg/kg ketamine was given supplemental when required to maintain surgical plane of anaesthesia (lack of pedal reflex). Body temperature was maintained with a supplemental heat source during the procedure. Animals were immediately euthanized after data acquisition was complete. All procedures involving animals were approved by the Cleveland Clinic Institutional Animal Care and Use Committee and in accordance with the NIH Guide for the Care and Use of Laboratory Animals.

2.5 Cell culture

Human microvascular endothelial cells (HMECs) (Catalogue # CRL-3243, ATCC, Manassas, VA, USA) were maintained in MCBD 131 medium (Catalogue # 10372019, Thermofisher, Waltham, MA, USA) + 10% FBS (Catalogue # 26140, Thermofisher, Waltham, MA, USA) + 100 U/mL penicillin/streptomycin (Catalogue # 15140122, Thermofisher, Waltham, MA, USA) + 2 mM L-Glutamin (PAA laboratories, Toronto, Ontario, Canada) + 0.05 mg/mL Hydrocortison. HMECs were used for experiments until the 15th passage. Immediately prior to TMAO exposure, HMECs were serum-starved for 1 h and exposed to the indicated concentrations of TMAO (Catalogue #317594, Sigma, St. Louis, MO, USA) for various time points, as indicated in the figure/legend. Human monocytic cells (THP-1) (Catalogue # TIB-202, ATCC, Manassas, VA, USA) were grown in RPMI 1640 medium (Catalogue # 12633012, Thermofisher, Waltham, MA, USA) + 10% FBS + 1% penicillin/streptomycin. THP-1 cells were exposed to 200 μM TMAO for 2 h.

2.6 RNA extraction and quantitative polymerase chain reaction (PCR)

For real-time polymerase chain reaction (PCR), total mRNA was isolated from cultured cells and murine tissue with TRIzol™ Reagent (Catalogue # 15596026, Thermofisher, Waltham, MA, USA) or peqGOLD TriFast (Catalogue # 30-2010, VWR Peqlab, Radnor, PA, USA). Aortic tissue was lysed using a tissue homogenzier (TissueLyser II, Quiagen, Hilden, Germany). Total RNA was transcribed to cDNA with the High-Capacity cDNA Reverse Transcription Kit (Catalogue # 4368814, Thermofisher, Waltham, MA, USA). Gene expression was determined using TaqMan Fast Universal PCR Master Mix (Catalogue #4366072, Thermofisher, Waltham, MA, USA) or TaqMan™ RNA-to-CT™ 1-Step Kit (Catalogue #4392653, Thermofisher, Waltham, MA, USA) using the following FAM- or VIC-tagged TaqMan® gene expression assays (all from Life Technologies, Carlsbad, CA, USA): Human GAPDH (Assay ID Hs99999905_m1), human asTF and flTF (Custom probes, for details see Reference[57]) human VCAM1 (Assay ID Hs01003372_m1), mouse GAPDH (Assay ID Mm99999915_g1), mouse flTF (Assay ID Mm00438856_m1), mouse asTF (custom probe, Clone ID AP7DRF4), mouse VCAM1 (Assay ID Mm00449197_m1). Relative gene expression was determined via the comparative C(t) (ΔΔCt) method with GAPDH as endogenous control for mRNA expression.

2.7 Western blot and ELISA

Cells and tissue samples were lysed in cell lysis buffer (10% glycerol, 10% SDS, pH adjusted to 7.6 using Tris) containing a protease/phosphate inhibitor cocktail (Catalogue # 5872, Cell Signaling, Danvers, MA, USA). Mouse aortas were homogenized using a Dual Tissue Grinder (DWK Life Sciences, Millville, NJ, USA) in 10 μL lysis buffer per 1 mg of tissue using zirconium oxide beads (Catalogue # 13765, Cayman Chemicals, Ann Arbor, MI, USA). Following quantification of protein with a BCA protein assay kit (Catalogue # 23225, Thermofisher, Waltham, MA, USA), homogenate was subjected to western blot as described previously.[57] For detection in mouse aortae, proteins were transferred to a Polyvinylidene fluoride membrane (Catalogue # IPFL00005, Merck Millipore, Burlington, MA, USA) and band intensity scanned using the Odyssey ImagingSystem (LiCor Inc, Lincoln, NE, USA). The following antibodies were used for detection: Goat anti-human TF (Catalogue # 4501, 4 μg/mL, American Diagnostica, Stamford, CT, USA), Goat anti-human asTF (Pineda, 1 μg/mL), Rabbit anti-human VCAM1 (Catalogue # 13662, 0.6 μg/mL, Cell Signaling, Danvers, MA, USA), Mouse anti-GAPDH (Catalogue # CB1001, 0.6 μg/mL, Calbiochem, San Diego, CA, USA), Rabbit Anti-mouse TF (Catalogue #4501, 2 μg/mL Biomedica, Vienna, Austria), Goat anti-VCAM1 (Catalogue #AF643, 1 μg/mL, R&D systems, Minneapolis, MN, USA), Mouse anti-GAPDH (Catalogue # MA5-15738, 0.1 μg/mL, Invitrogen, Carlsbad, CA, USA,), 680RD Donkey anti-Goat IgG (Catalogue # 926-68074, 0.1 μg/mL, LiCor Inc, Lincoln, NE, USA), 680RD Goat anti-Rabbit IgG (Catalogue # 926-68071, 0.1 μg/mL, LiCor Inc, Lincoln, NE, USA), and 800CW Goat anti-Mouse IgG (Catalogue # 926-32210, 0.1 μg/mL, LiCor Inc, Lincoln, NE, USA). Recombinant mouse TF (Catalogue # RPA524Mu01, 1 ng, Cloud-Clone Corp, Houston, TX, USA) was used as a positive control. ImageJ (NIH) software was used to quantify images.

TAT levels in mouse plasma were assessed by using Siemens Enzygnost® TAT micro immunoassay (Catalogue # OWMG15 Siemens, Erlangen, Germany).

2.8 Immunohistochemistry and immunofluorescence of mouse tissue

Frozen sections of aortas and carotid arteries were mounted on glass slides, fixed with IC fixation buffer (Catalogue # 00-8222-49 Invitrogen, Carlsbad, CA, USA) for 20 min, and washed three times in dH_2O. After quenching endogenous peroxidase with 3% H_2O_2 (Fisher Chemical, Catalogue # 7722-84-1) for 10 min, non-specific avidin-biotin activity was blocked with an avidin/biotin blocking kit (Catalogue #SP-2001, Vector laboratories, Burlingame, CA, USA). Sections were then blocked with normal Rabbit Serum Blocking reagent (Catalogue # S-5000, Vector laboratories, Burlingame, CA, USA) for 1 h followed by overnight incubation with the primary antibodies: rat anti-TF 1H1 8 μg/mL, rat IgG2a κ isotype control (clone eBR2a, 8 μg/mL, eBioscience San Diego, CA, USA), rat anti-mouse VCAM1(CD106) (Catalogue # 550547, 0.62508 μg/mL BD Pharmingen, San Diego, CA, USA), goat anti-CD31 (AF3628, 15 μg/mL, R&D systems, Minneapolis, MN, USA), and rat anti-mouse CD41 (clone MWReg3, 10 μg/mL, BD Pharmingen, San Diego, CA, USA). The slides were developed by Vectastain Elite ABC (Catalogue # PK-6105, Vector laboratories, Burlingame, CA, USA) with 3,3'-diaminobenzidine (DAB) (Catalogue # SK-4100, Vector laboratories, Burlingame, CA, USA) or 3-amino-9-ethylcarbazole (AEC, Catalogue # K3464, Dako, Jena, Germany) and then counterstained with haematoxylin (Catalogue # H-3401, Vector laboratories, Burlingame, CA, USA) and mounted in Aqua-Poly/Mount medium (Catalogue # NC9439247, Polysciences, Warrington, PA, USA). Images were taken using a light microscope (Olympus type BX61). Quantification was performed using the software QuPath0.2.0-m10.[58] Background values were adjusted by measuring average background within each image to minimize error due to minor intensity variations across the image set. DAB and AEC signals were isolated using the colour deconvolution function

of QuPath.[58] Mean optical density (OD) for DAB or AEC stain was quantified by manually annotating the endothelial layer or thrombus and mean OD quantified within the endothelial layer or thrombus. Three distinct anatomic sides per animal were quantified with mouse aortas including both thoracic and abdominal parts.

For immunofluorescence, aortic tissue was blocked with the avidin/biotin blocking kit (Catalogue # SP-2001, Vector laboratories, Burlingame, CA, USA) and 10% normal goat serum (Catalogue # X0907, DAKO, Jena, Germany). Analysis was performed with the following antibodies/probes: rat anti-TF 1H1 (8 μg/mL), rabbit anti-mouse TF (Catalogue # 4501, 10 μg/mL, Biomedica, Vienna, Austria), rat anti-mouse VCAM1 (Catalogue # 550547, 0.625ug/mL, BD Pharmingen, San Diego, CA, USA), rabbit anti-mouse VCAM1 (Catalogue # 39036, 1:1000 dilution, Cell Signaling, Danvers, MA, USA), goat anti-CD31 (AF3628, 15ug/mL, R&D systems, Minneapolis, MN, USA), Goat IgG anti-Rabbit IgG-Biotin (Catalogue # 111-065-045, 6 μg/mL Dianova), biotinylated rabbit anti-rat IgG Antibody

(Catalogue # BA-4000, Vector laboratories, Burlingame, CA, USA), Streptavidin-Cy3 (Catalogue # 016-160-084, 7 μg/mL, Dianova, Hamburg, Germany), Streptavidin DyLight® 549 (Catalogue # SA-5549-1, 1 μg/mL Vector laboratories, Burlingame, CA, USA), Alexa 488 donkey anti-goat (Catalogue # A11055, 4 μg/mL, Invitrogen, Carlsbad, CA, USA), Alexa 647 donkey anti-rabbit IgG (Catalogue # A31573, 4 μg/mL, Invitrogen, Carlsbad, CA, USA), DAPI (Catalogue # D1168, 2 μg/mL, Invitrogen, Carlsbad, CA, USA), and Phalloidin–Atto 647 N (Catalogue # 65906, 0.02 μM, Thermofisher, Waltham, MA, USA).

2.9 Caecal microbiota composition analyses and statistical analysis

The 16S rRNA gene sequencing methods used were adapted from the methods developed for the National Institutes of Health-Human Microbiome Project.[59] Briefly, genomic DNA was extracted from individual mouse caecum with a MagAttract HMW DNA Kit (Qiagen, Hilden, Germany). Next, the 16S rRNA V4 region was amplified and sequenced on Illumina Iseq 100 platform following the manufacturer's instructions. Raw 16S amplicon sequence (forward reads only) and metadata were demultiplexed using the split_libraries_fastq.py script implemented in QIIME1.9.1.[60] The demultiplexed fastq file was split into sample-specific fastq files using split_sequence_file_on_sample_ids.py script from Qiime1.9.1.[60] Individual fastq files without non-biological nucleotides were processed using Divisive Amplicon Denoising Algorithm pipeline.[61] The output of the dada2 pipeline (feature table of amplicon sequence variants) was processed for alpha and beta diversity analysis using phyloseq[62] and microbiomeSeq (http://www.github.com/umerijaz/microbiomeSeq) packages in R. Alpha diversity estimates were analysed within group categories using estimate_richness function of the phyloseq package.[62] Non-multidimensional scaling (NMDS) was performed using Bray–Curtis dissimilarity matrix37[63] between groups and visualized by using ggplot2 package. We assessed the statistical significance ($P < 0.05$) throughout and whenever necessary adjusted P-values for multiple comparisons according to the Benjamini and Hochberg method to control false discovery rate,[64] while performing multiple testing on taxa abundance according to sample categories. We performed an ANOVA among sample categories while measuring α-diversity using the plot_anova_diversity function in microbiomeSeq package (http://www.github.com/umerijaz/microbiomeSeq). Permutational multivariate ANOVA with 999 permutations was performed to test the statistical significance of the NMDS patterns with the ordination function of the microbiomeSeq package. Linear regression was performed on taxa abundances against metadata variables using 'lm' function implemented in dplyr package in R.

Statistical analyses were performed using the software GraphPad Prism 8 and R 3.5.3 (Vienna, Austria, 2018). For the clinical analysis, Shapiro–Wilk test was used to test for normality. Continuous data are presented as mean ± standard deviation or median (interquartile range), categorical variables are presented as %. Hazards ratios (HR)s for incident MACE at 1 and 3-years follow-up and corresponding 95% confidence interval (95% CI) were analysed using univariable (unadjusted) and multivariable (adjusted) Cox models. Kaplan–Meier analysis with Cox proportional hazards regression was used for event-free survival from MACE. Adjustments were made for traditional cardiac risk factors including age, sex, hypertension, smoking, diabetes, HDL cholesterol, LDL cholesterol, and triglycerides (adjustment 1); and all of the above mentioned adjustments in addition to creatinine levels (adjustment 2).

In cell culture and animal experiments, the D'Agostino–Pearson test was applied to test for normality. After testing for normal distribution, differences between two groups were examined using either a Student's *t*-test or Mann–Whitney test (non-parametric). For comparisons of one parameter between more than two related groups, an ANOVA with Tukey's multiple comparisons test (parametric) or a Kruskal–Wallis test with Dunn's multiple comparison *post hoc* test (non-parametric) was performed. For correlation between plasma TMAO levels and vascular TF and VCAM expression, P-values were calculated using non-parametric Spearman correlation. *In vitro* laboratory and animal model data are represented as mean ± SEM. P-values < 0.05 are considered statistically significant.

3. Results

3.1 Plasma TMAO levels are associated with incident major adverse cardiovascular events in patients on anti-platelet therapy

TMAO directly enhances platelet stimulus-dependent intracellular calcium release, reactivity and thrombosis.[22,24,38] We reasoned that if elevated TMAO levels foster a pro-thrombotic effect in subjects partially via TF pathway activation, we should find associations between circulating TMAO levels and thrombotic events even among subjects on anti-platelet therapy. To test this, we analysed two large independent cohorts of varying patient risk profile: (i) the first comprised of a single-centre cohort of stable patients undergoing elective diagnostic coronary angiography (including both primary and secondary prevention patients) (Cleveland Clinic GeneBank). In the present analyses, only the subset of GeneBank subjects treated with anti-platelet therapy (primarily aspirin) throughout longitudinal follow-up were included ($n = 2989$); (ii) the second cohort is comprised of a multi-centre observational study of patients presenting with ACS. In the present analyses, only the subset of subjects treated with dual anti-platelet therapy throughout longitudinal follow-up were included (Swiss ACS, $n = 1469$). Baseline characteristics for each cohort are shown in Supplementary material online, *Tables S1 and S2*.

Kaplan–Meier analyses revealed an increase in event (MACE) rates with increasing TMAO quartiles among GeneBank subjects on anti-platelet therapy (defined as either aspirin or ADP-receptor antagonists) (log rank $P < 0.0001$) (*Figure 1A*). This association was also observed when restricting analyses to individuals on aspirin alone throughout the

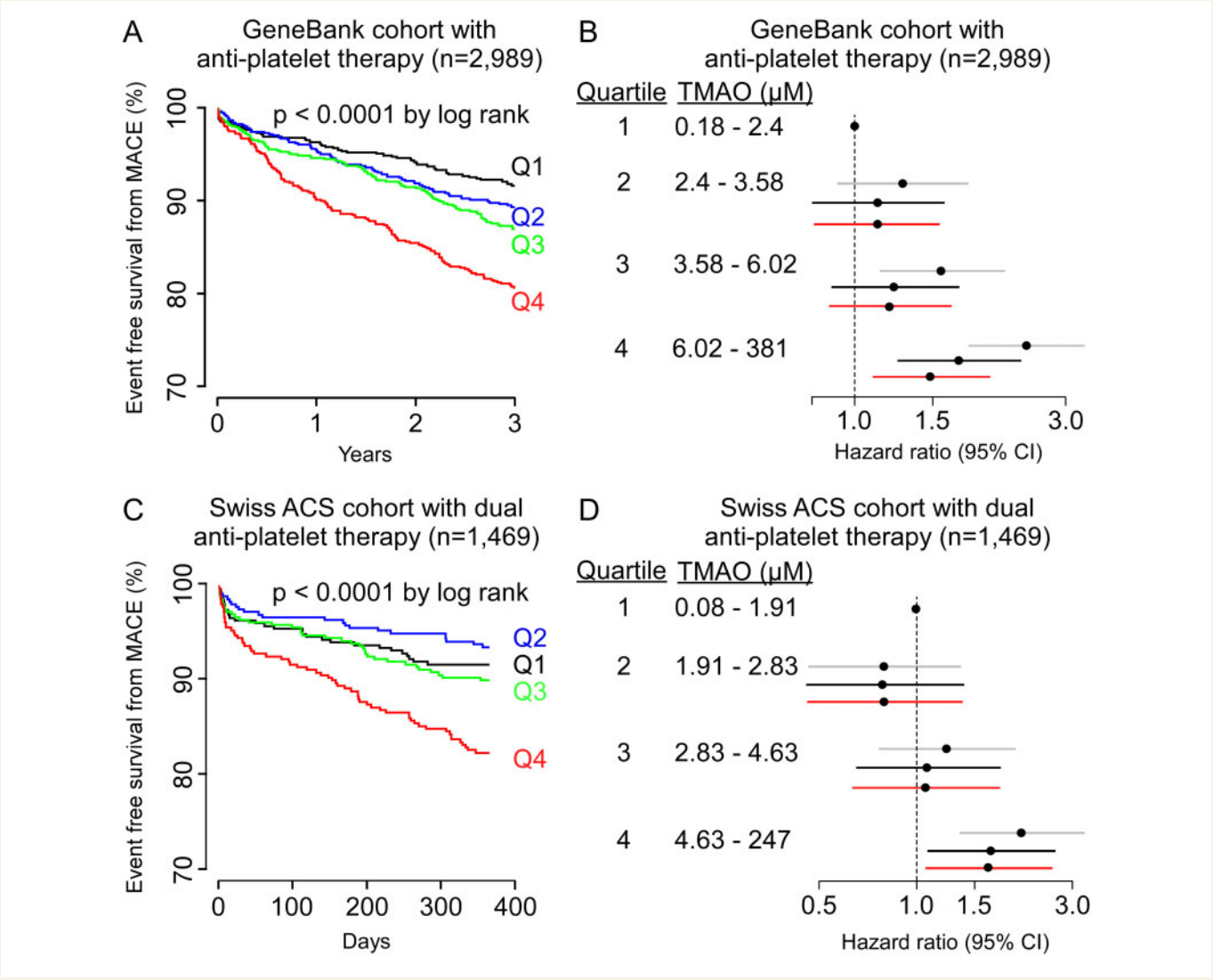

Figure 1 The association of TMAO levels with thromboembolic clinical outcomes in patients on anti-platelets in the Cleveland and Swiss ACS Cohorts. Kaplan–Meier estimates and the risk of incident MACE (MI, stroke, or death) over follow-up periods ranked by quartiles of TMAO levels in (*A*) GeneBank patients with anti-platelet therapy (aspirin or ADP-receptor antagonists) as well as (*C*) Swiss ACS patients with dual anti-platelet therapy. *P*-values by log rank test are indicated. Forest plots indicating the risks of (*B*) incident MACE at 3 years for GeneBank and (*D*) at 1 year for Swiss ACS subjects stratified by quartiles of TMAO levels (unadjusted in grey), multivariable Cox model for HR included adjustments for traditional risk factors including age, gender, hypertension, smoking, diabetes, HDL, LDL, TG (adjustment 1, in black); and traditional risk factors plus renal function (adjustment 2, in red), as described in Section 2. The 5–95% CI is indicated by line length.

follow-up period (log rank $P < 0.0001$, $n = 2793$, Supplementary material online, *Figure S1A*). Multivariable Cox models with adjustments for traditional risk factors (including age, sex, hypertension, smoking, diabetes, HDL cholesterol, LDL cholesterol, and triglycerides; adjustment 1), including additional adjustments for renal function (adjustment 2), showed elevated TMAO remained significantly associated with incident MACE in all subjects on anti-platelet therapy [HR 95% CI for quartile (Q)4 vs. Q1, 1.73 (1.25–2.38), $P = 0.0008$ and 1.50 (1.08–2.10), $P = 0.0157$, respectively, *Figure 1B*], as well as subjects on aspirin only [1.75 (1.25–2.44), $P = 0.0012$, Supplementary material online, *Figure S1B*].

We next sought to determine whether the strong prognostic value of TMAO in stable subjects on anti-platelet therapy observed in the single-centre Cleveland (GeneBank) cohort could be replicated in an independent cohort of patients with heightened risk profile. For this, we elected to examine TMAO levels in patients presenting with ACS in the independent multi-site SPUM-ACS cohort, examining the subset ($n = 1469$) of patients who were treated with DAPT throughout the 1-year follow-up period, as described in Section 2. Again, Kaplan–Meier survival analyses revealed increasing TMAO levels were associated with a graded increase (log rank $P < 0.0001$) in incident MACE (*Figure 1C*). Moreover, patients with higher TMAO levels (e.g. Q4 vs. Q1) showed a significant 2.1-fold increase in incident MACE risk [HR (95% CI) at 1 year of 2.1 (1.35–3.28), $P = 0.001$], which remained significant after adjustment for traditional risk factors as above, as well as with adjustments for traditional risk factors plus renal function [1.70 (1.08–2.69), $P = 0.02$ and 1.67 (1.05–2.64), $P = 0.0302$, respectively, *Figure 1D*]. While clinical association studies such as these cannot directly demonstrate mechanism of action, they nonetheless can serve as hypothesis generation studies. The results

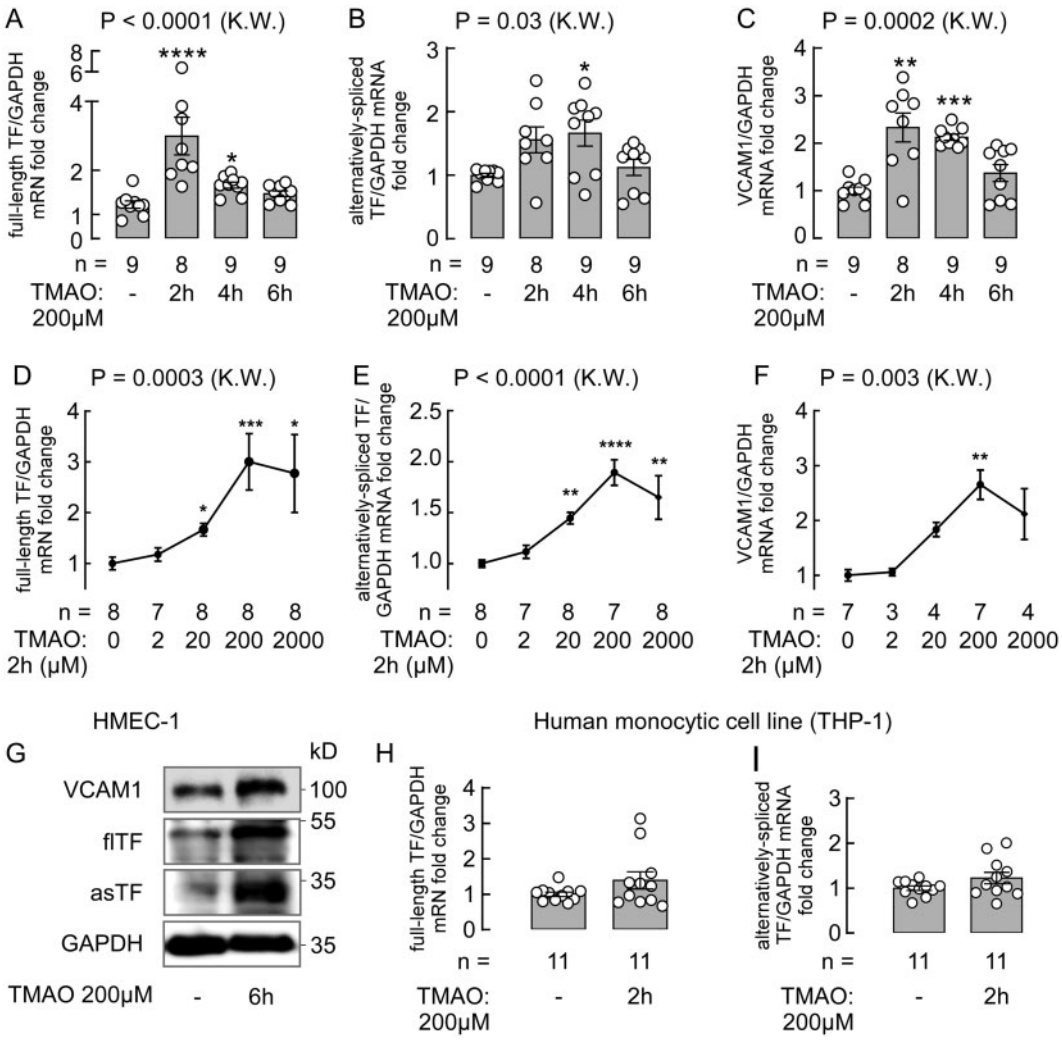

Figure 2 Effects of TMAO exposure on TF and VCAM1 expression in human endothelial cells. HMEC-1 was left untreated or exposed to 200 μM TMAO for 2, 4, and 6 h and mRNA expression for (*A*) flTF, (*B*) asTF, and (*C*) VCAM1 analysed. In addition, HMEC-1 was treated with vehicle or TMAO at different concentrations as indicated for 2 h and mRNA expression of (*D*) flTF, (*E*) asTF, and (*F*) VCAM1 assessed. (*G*) Protein amounts of flTF, asTF, and VCAM1 in HMEC treated with 200 μM TMAO for 6 h quantified via western blot. Human monocytic THP-1 cells were treated with TMAO or vehicle for 2 h and mRNA expression of (*H*) flTF and (*I*) asTF analysed. Results are presented as mean±SEM. Global *P*-values shown were obtained by non-parametric Kruskal–Wallis test with Dunn's multiple comparisons *post hoc* test to compare different treatments. Differences between two groups were assessed using a Mann–Whitney test. **P* < 0.05, ***P* < 0.01, ****P* < 0.001, *****P* < 0.0001.

arguably suggest that factors independent of a direct effect of TMAO on platelet reactivity are likely involved in the observed residual clinical risks since TMAO remained associated with increased MACE even in the presence of anti-platelet agents. Moreover, multiple prior mechanistic investigations have demonstrated that TMAO enhances *in vivo* thrombosis in animal models.[5,19,22,24,38–40]

3.2 TMAO induces expression of TF and VCAM1 in HMECs

We used HMEC-1 as a model system to test the hypothesis that the gut microbiota-derived metabolite TMAO impacts vascular TF expression and adhesion molecules that are induced by activated endothelial cells. Notably, TMAO induced a robust induction of *TF* mRNA (both flTF and asTF), and *VCAM1* mRNA in HMEC-1 after 2–4 h of incubation (*Figure 2A–C*). Dose–response experiments demonstrated that physiological TMAO concentrations (within the ranges observed in both of our patient cohorts, *Figure 1*; and in reported clinical studies[28–31]) were sufficient to induce both *TF* isoform transcripts and *VCAM1* mRNA expression (*Figure 2D–F*). Western blot experiments confirmed the TMAO-dependent expression of endothelial flTF, asTF, and VCAM1 on the protein level (*Figure 2G*). By contrast, TMAO had no effect on TF expression in human monocytic (THP-1) cells (*Figure 2H and I*).

3.3 Acute elevation of TMAO induces aortic endothelial TF and VCAM1 expression *in vivo*

We used mouse models to analyse the effects of acute TMAO exposure on aortic TF and VCAM1 expression *in vivo*. For this purpose, C57/BL6

mice were injected intraperitoneally with TMAO or vehicle, and both blood and aortas were harvested either 1.5 h or 6 h post injection to assess plasma TMAO levels and aortic *TF* mRNA and protein expression. Analyses of samples collected 1.5 h post-TMAO injection (compared to controls) showed an increase in circulating TMAO levels (*Figure 3A*) without elevation in its precursor metabolite TMA (Supplementary material online, *Figure S2A*). At this time point post injection, the TMAO increase was accompanied by induction of both *flTF and asTF* mRNA, but not *VCAM1* mRNA (*Figure 3B–D*). Moreover, we observed a correlation of plasma TMAO levels with flTF expression, but not with asTF (Spearman R 0.66, $P = 0.04$ for flTF, Supplementary material online, *Figure S2B and C*). When blood and aortic tissues were examined 6 h following intraperitoneal injection of either TMAO or vehicle, a much lower elevation in plasma TMAO was observed (*Figure 3E*), whereas western blot analysis of aortic lysates showed a significant increase in TF protein and a trend towards more VCAM1 protein (*Figure 3F and G*). Immunohistochemistry studies of aortic sections localized both TF and VCAM1 to the endothelial layer (*Figure 3H*).

3.4 A chronic elevation in TMAO levels with choline-supplemented diet induces aortic TF and VCAM1 expression

We next assessed the impact of chronic increases in TMAO levels on vascular TF and VCAM1 expression using dietary manipulation. C57/BL6 mice were fed either a chemically defined diet (chow) or the same diet supplemented with choline (1% choline) for 10 days, and then blood and tissues were recovered for analyses as described under Section 2. As expected, chronic dietary choline supplementation led to a significant increase in plasma levels of choline, TMA (Supplementary material online, *Figure S3A and B*) and TMAO (*Figure 4A*). Higher plasma TMAO was associated with increased aortic *flTF* mRNA expression but not *asTF*, and a trend for increased RNA levels of *VCAM1* that failed to reach statistical significance (*Figure 4B–D*). Notably, western blot analyses of aortic lysates revealed significant choline diet-induced increases in both TF and VCAM1 protein (*Figure 4E and F*). In line with our finding that TMAO failed to induce TF in human monocytes (*Figure 2H and I*), we observed no difference in TAT in citrated plasma recovered from mice supplemented with choline vs. the control (chow) diet, suggesting that mouse monocytic TF production[65] is not induced by TMAO (*Figure 4G*). Parallel immunohistochemistry studies using the well-established 1H1 anti-TF antibody[55] and a VCAM1-specific antibody (Section 2) revealed that dietary supplementation with choline resulted in both chronic TMAO elevation and induction of both TF and VCAM1 vascular protein. Moreover, immunolocalization studies showed staining primarily within the endothelial layer of the aorta, as judged by co-localization with endothelial cell-specific marker CD31 (*Figure 4H and I* and Supplementary material online, *Figure S4*). The endothelial localization of vascular wall TF and VCAM1 (induced by a choline-supplemented diet) was also further confirmed in immunofluorescence studies with double staining of CD31 with either TF or VCAM1 (Supplementary material online, *Figure S4*).

3.5 Pharmacological targeting of gut microbial choline TMA-lyase prevents TMAO-related vascular TF and VCAM1 expression in the host

In additional studies, we analysed the effect of a recently developed and characterized non-lethal (with respect to microbes; i.e. non-antibiotic) small molecule inhibitor FMC—which specifically targets microbial choline TMA-lyases—on host vascular TF expression.[39] FMC was designed as a mechanism-based inhibitor that both selectively accumulates within gut microbiota and is poorly absorbed in the host.[39] C57/BL6 mice were fed a choline-supplemented diet with or without FMC in the drinking water. Provision of FMC drastically reduced circulating TMA and TMAO (>95%), while enhancing choline bioavailability (*Figure 5B*). Aortas of animals on the choline-supplemented diet showed strong immunohistochemical staining localized to the aortic endothelium using distinct mAb specific for either TF (*Figure 5A*, upper left panel) or VCAM1 (*Figure 5A*, middle left panel). By contrast, immunostaining of aortas recovered from choline diet-supplemented littermates that also received FMC showed virtually undetectable aortic endothelial TF or VCAM1 (*Figure 5A*, upper and middle right panel). Notably, FMC treatment did not change the extent of perivascular (interstitial) TF protein. Computer image analysis of multiple sections of tissue staining across three distinct anatomic sides per animal (as described under Section 2) revealed a significant increase in both TF and VCAM1 protein under conditions where TMAO levels were elevated (*Figure 5B*). In Addition, Spearman correlation analyses demonstrated significant associations between circulating TMAO or TMA levels with either endothelial cell TF (*Figure 5C* left panel) or VCAM1 (*Figure 5C*, right panel).

3.6 Infusion of an inhibitory anti-TF antibody prevents TMAO-enhanced thrombosis potential *in vivo*

To assess the role of TMAO-depending vascular TF expression on thrombus formation *in vivo*, we conducted a proof-of-concept study using the carotid artery injury ($FeCl_3$) model. Animals were chronically fed a chemically defined diet (chow) with experimentally determined total choline content (0.08 g%) vs. the same diet supplemented with 1.0 g% choline (choline diet, total choline content 1.08 g%). After 2 weeks of choline supplemented diet, the impact of TF inhibition on TMAO-enhanced *in vivo* thrombosis potential was examined. For these studies, mice on the choline diet were randomly split into either treatment with the rat anti-mouse TF monoclonal antibody[55] or isotype-matched rat IgG2a κ control antibody (clone eBR2a, eBioscience San Diego, CA, USA), as described in Section 2, before quantifying both $FeCl_3$ injury-induced *in vivo* thrombus formation and time to cessation of blood flow in the injured arterial segment. Fluorescent micrographs of the growing thrombus over time from a representative mouse from each group are shown in *Figure 6A*, and quantitation of time to cessation of blood flow in all animals is shown in *Figure 6B*. Review of the representative fluorescent images of the growing thrombus readily reveal that mice fed a choline-supplemented diet (receiving control IgG2a treatment) have more rapid $FeCl_3$-induced thrombus formation compared to chow-fed animals, as well as marked reduction in time to vessel occlusion (*Figure 6A*). Strikingly, despite maintaining a comparably high TMAO level, mice on the choline diet that were administered the TF-inhibitory antibody (1H1) showed marked reversal of both the TMAO-enhanced thrombus formation (*Figure 6A*) and TMAO-reduced time to cessation of blood flow, with occlusion times nearly normalized to what was observed in chow-fed animals (*Figure 6B*). Immunohistochemistry examination was also performed on the injured carotid arteries with thrombi recovered from animals injected with the control IgG2a (N.B. the anti-TF antibody injected i.p. is the same antibody as used in immunohistochemical examination, preventing examination of tissues recovered from mice already injected with the inhibitory antibody). Notably, the choline diet-fed mice exhibited more endothelial TF that was incorporated into the thrombus

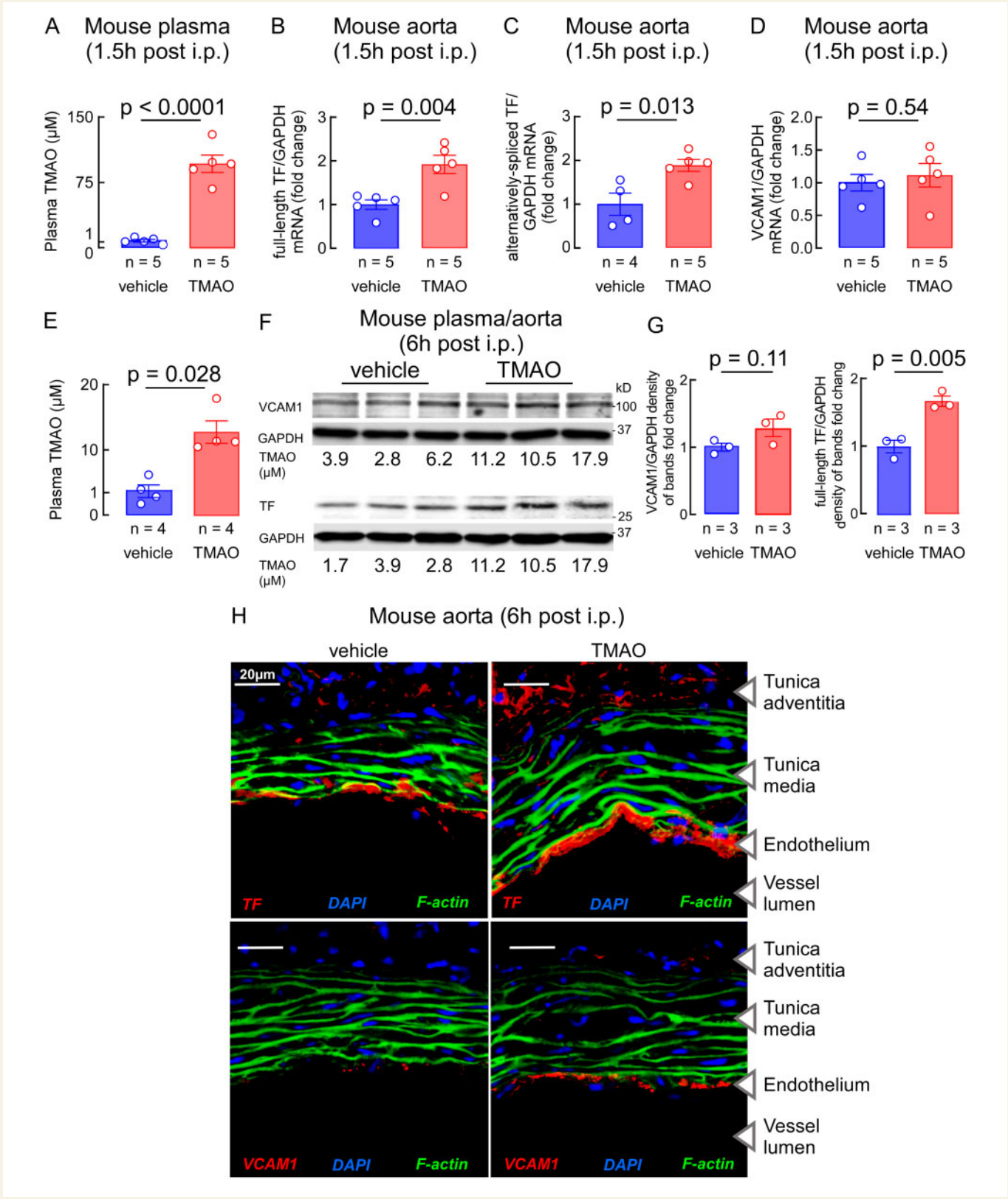

Figure 3 TMAO acutely raises TF and VCAM1 expression in aortic tissue *in vivo*. C57/BL6 mice were injected with TMAO or vehicle intraperitoneally for 1.5 h. Next, (*A*) plasma TMAO levels were quantified by LC/MS/MS and arotic mRNA expression of (*B*) flTF, (*C*) asTF, and (*D*) VCAM1 quantified via TaqMan rtPCR. To assess protein expression, the animals were injected with vehicle or TMAO for 6 h. Subsequently, (*E*) TMAO plasma levels and (*F*) protein amounts of TF and VCAM1 were quantified via western blot and (*G*) density of the protein bands quantified. (*H*) To analyse localization within the vessel wall, aortic tissue of TMAO-injected mice was probed for TF and VCAM1 expression 6 h post injection using immunofluorescence staining (TF red, upper panel, VCAM1 red, lower panel). The tissue was counterstained with DAPI (blue) and an f-actin probe (green). Results are presented as mean±SEM. Pairwise comparison was performed using a Mann–Whitney test.

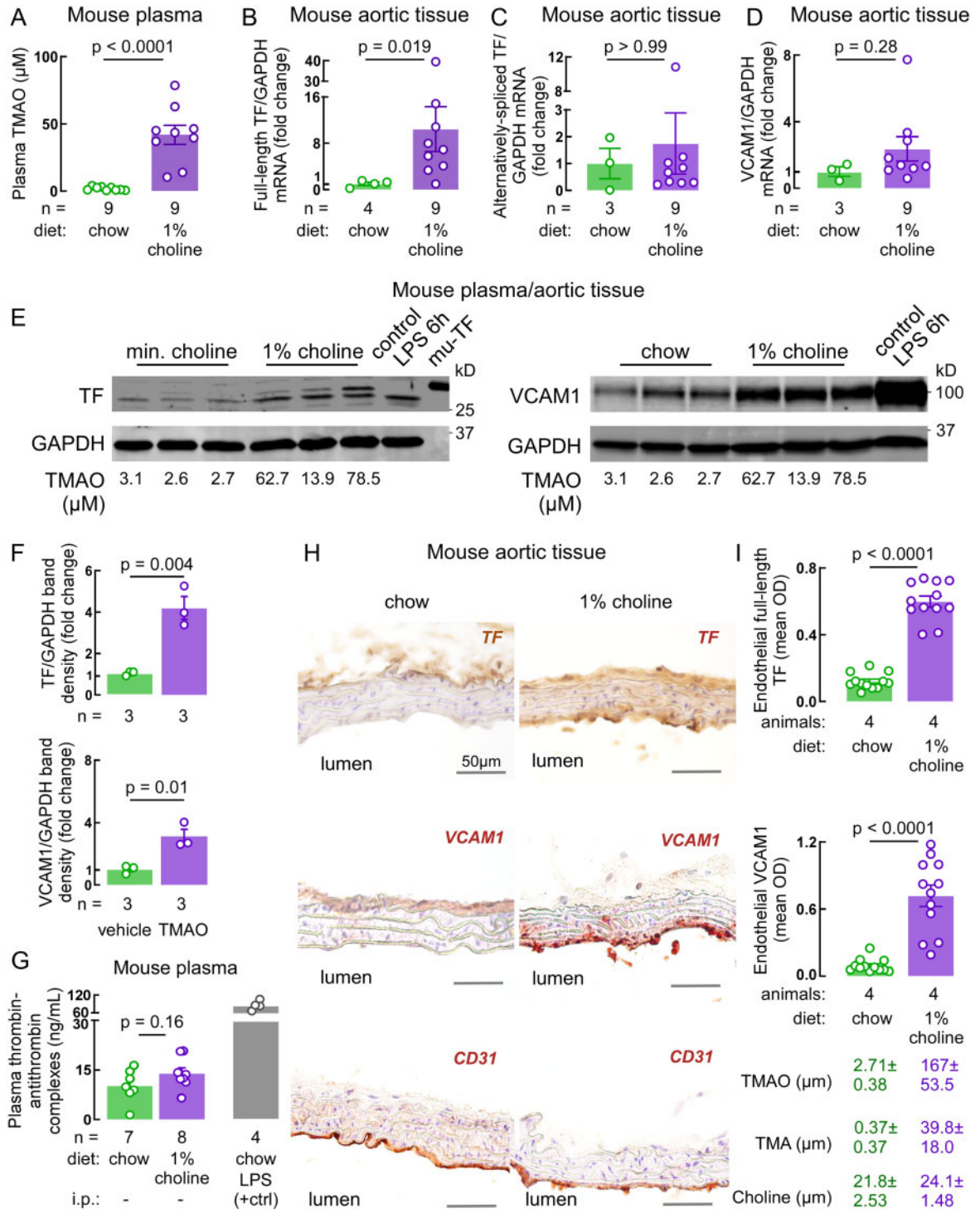

Figure 4 TMAO chronically induces endothelial TF and VCAM1 expression in mouse aortas *in vivo*. C57/BL6 mice were either fed a control chow diet or a choline diet. After 10 days of diet, (*A*) plasma levels of TMAO were quantified and aortic mRNA expression for (*B*) flTF, (*C*)asTF, and (*D*) VCAM1 analysed. (*E*) Protein amounts of TF and VCAM1 in aortic tissue were measured via western blot and related to the corresponding plasma levels of TMAO. Aortas of LPS-injected mice (15 mg/kg for 6 h) as well as recombinant mouse TF were used as positive controls. (*F*) Density of the detected bands was quantified using an imaging software. (*G*) Plasma of the same animals was analysed with respect to TAT complexes via ELISA. LPS-injected animals served as a known positive control for TAT induction (*H*) Immunohistochemistry experiments using specific antibodies were used to assess protein expression of TF, VCAM1, and the endothelial marker CD31 in aortic tissue. (*I*) Mean OD of endothelial protein expression from three different anatomical sides was quantified using an imaging software and three data points for each animal were plotted. Results are presented as mean±SEM. Pairwise comparison was performed using a Mann–Whitney test.

(*Figure 6C and D*). Moreover, thrombi were seen to be mainly composed of platelets, as evidenced by a CD41-specific staining, with a modest increase in choline-fed animals as compared to chow-fed littermates (*Figure 6C and D*).

3.7 The gut microbiota choline TMA-lyase inhibitor, FMC, modulates TMAO-associated taxa and their association with vascular TF and VCAM1 expression

In parallel studies, we examined the impact of a choline diet and FMC treatment on gut microbial community structure with respect to TMAO-associated taxa, and their association with vascular TF and VCAM1 expression. Caecal microbial DNA encoding *16S* ribosomal RNA was sequenced, and NMDS was performed among the groups of mice. Shannon index-based alpha diversity analyses revealed significant differences between the groups (*Figure 7A*). Three distinct (non-overlapping) clusters in the principal component analysis (*Figure 7B*) indicated that dietary choline and dietary choline + FMC each induced significant (permutational multivariate ANOVA, $R^2 = 0.67$, $P = 0.001$) detectable rearrangements in the overall caecal microbial composition. Notably, we identified multiple caecal microbial taxa whose abundances accounted for significant ($P < 0.05$, Benjamini Hochberg false discovery rate corrected) differences observed among the different groups (chow, choline, and choline+FMC) (*Figure 7C*).

In additional analyses, we also tested whether the proportions of the taxa that changed upon different treatments were significantly correlated with TMAO or expression of either vascular TF or VCAM1, the latter two quantified by immunohistochemical OD analyses (Section 2) in the endothelial layer of aortic tissue sections. The caecal microbial community of choline diet-fed animals showed a significant increase in the proportion of the genera *Dorea and Candidatus stoquefichus*, whose proportion was reduced by exposure to FMC close to levels observed in mice fed the control (chow) diet (*Figure 7C*). Furthermore, the proportions of *Dorea and Candidatus stoquefichus* significantly correlated with plasma levels of TMAO and both vascular TF and VCAM1 expression levels. By contrast, a choline diet reduced the proportion of *Lachnospiraceae NK4136* and *Anaerotruncus*, whose proportions were restored (reduced) by FMC treatment to levels similar to those observed on chow (*Figure 7C*). These caecal microbiota genera also correlated significantly with plasma levels of TMAO, aortic endothelial cell TF, and VCAM1 immunohistochemical staining (*Anaerotruncus*). In line with our findings, *Lachnospiraceae* has previously been shown to be associated with lower TMAO levels and an anti-thrombotic phenotype.[22] Furthermore, significant correlations of additional genera with aortic tissue endothelial cell TF or VCAM1 levels were also observed for *Acetitomaculum, Oscillibater, Romboutsia, Roseburia, Ruminiclostridium, Ruminococcaceae*, and *Tucicibacter* (Supplementary material online, *Figures S5 and S6*).

4. Discussion

The TF pathway is the rate-limiting step for *in vivo* thrombosis. Moreover, adverse phenotypes that are linked to pathological vascular TF expression, including diabetes,[66–68] coronary artery disease,[69] myocardial infarction,[70,71] and stroke,[72] likewise show strong associations with elevated levels of TMAO.[7,23,53,73] Here, we show that TMAO induces vascular endothelial TF, which the present studies reveal contributes to TMAO-heightened thrombosis potential *in vivo*. Our studies thus provide new mechanistic insights into how the metaorganismal TMAO pathway and gut microbiota can contribute to atherothrombotic event risks. They also identify a new axis that enhances the risk for thrombosis, comprising diet, microbiome, TMAO, and vascular TF.

In multiple cohorts with varying clinical phenotypes ranging from stable subjects undergoing elective diagnostic coronary angiography to patients presenting with ACS, we observed heightened MACE risk with elevated TMAO levels, even in the presence of one or more anti-platelet drugs. Although prior studies have reported an association between TMAO and adverse outcomes in patient cohorts that include some individuals on anti-platelet agents—e.g. in secondary stroke prophylaxis[23] or following ACS[74]—there has been no analysis of TMAO's prognostic value in cohorts with documented anti-platelet therapy for all subjects throughout the duration of follow-up. The pathogenesis of thrombosis is complex and involves platelets, the vascular wall and coagulation factors. Our clinical findings suggest that factors within the vasculature in addition to platelets that are not inhibited by anti-platelet therapy contribute to the heighted thrombosis risk promoted by TMAO. While clinical studies that have quantified coronary atherosclerotic plaque using detailed quantitative coronary angiography and GENSINI score, or SYNTAX score, or optical coherence tomography, have shown an association between TMAO and both atherosclerotic plaque burden[75–77] and plaque vulnerability,[32,33] other studies examining different surrogate markers of plaque like coronary artery calcification and carotid intimal medial thickness have failed to observe an association.[35] Notably, multiple studies have reported a strong association between TMAO levels and increased arterial thrombotic events,[12,22,23,38,74] and a recent animal model study reported that circulating TMAO could reduce the inhibitory effects of clopidogrel on platelet aggregation.[78] Thrombus generation involves multiple cell types (vascular cells and platelets)[79] and biochemical pathways, including the extrinsic coagulation pathway.[80] Our prior studies on the TMAO pathway and thrombosis have primarily focused on the ability of TMAO to directly impact platelet calcium signalling, and the impact of TMAO on platelet responsiveness to a variety of agonists.[22,38] In addition, numerous studies have shown that TMAO can activate vascular endothelial cells through either NF-κB- or NLRP3-dependent pathways, providing additional potential mechanisms for TMAO-dependent enhancement of platelet adhesion and clot formation *in vivo*.[17,36,81–86] However, surprisingly, despite the clinical associations between TMAO and thrombotic event risks, and the central role of the TF pathway in both thrombosis and the extrinsic clotting cascade,[41,42] few studies have examined the relationship between TMAO and TF. One recent *in vitro* study with cultured vascular endothelial cells reported that TMAO addition to media up regulates TF expression.[87] However, no studies to date have examined whether an increase in TMAO directly leads to enhanced vascular TF expression *in vivo*, contributes to TMAO-dependent heightened thrombosis susceptibility in animal models, or is associated with MACE in patients on anti-platelet therapies.

While the present studies demonstrate a mechanistic link between TMAO and TF dependent increases in thrombosis susceptibility *in vivo*, further investigation is needed to understand the host signalling partners involved. Thus, it remains to be established what molecular participant(s) in the host link TMAO elevation to enhanced vascular endothelial cell TF expression. One candidate that merits further investigation is the recently reported TMAO receptor PKR-like ER kinase (PERK), a component of the protein unfolding response.[88] In that study, PERK was reported to bind to TMAO and trigger TMAO-dependent changes in glucose metabolism. However, its involvement in other more traditional

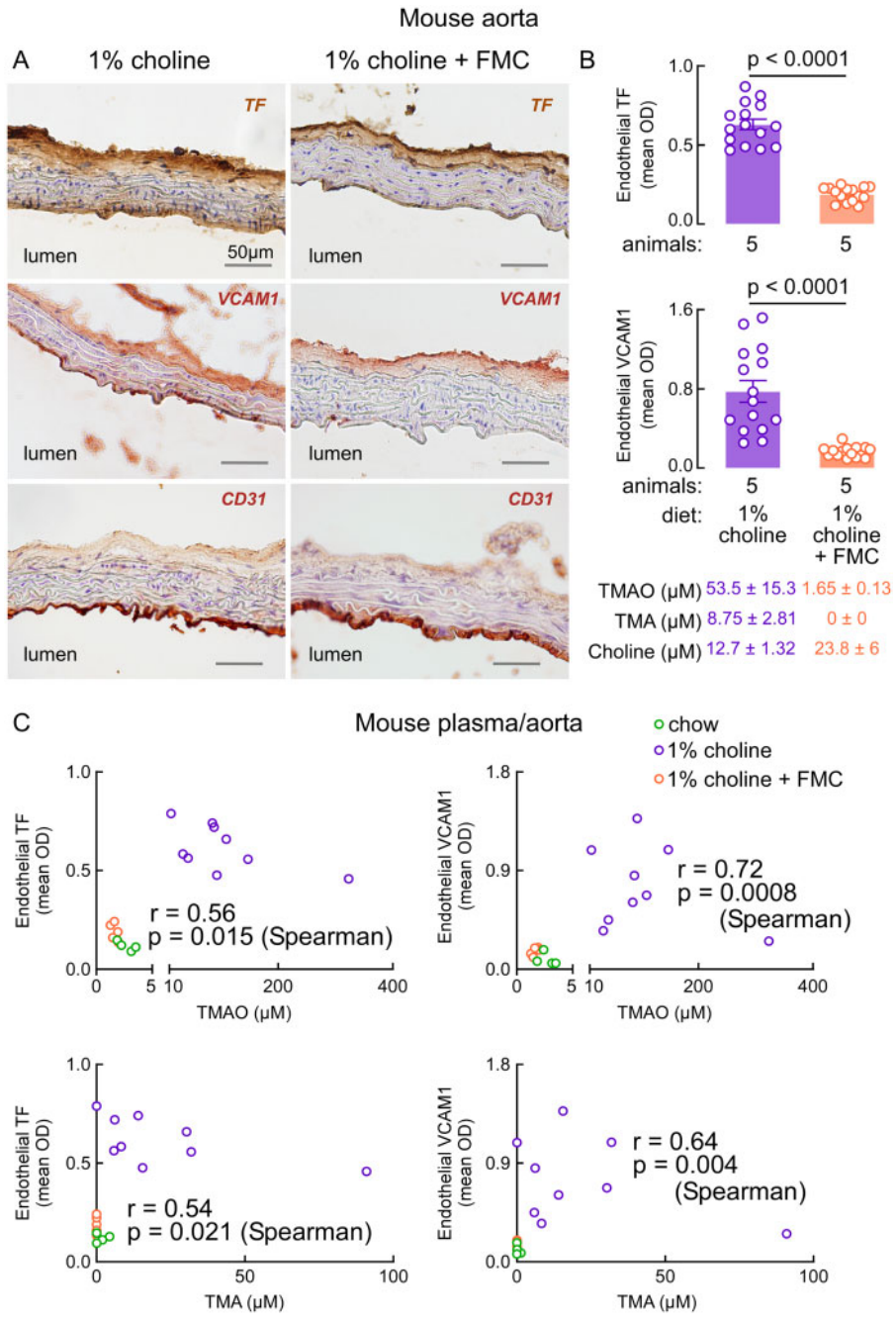

Figure 5 A small molecule TMA-lyase inhibitor reverses TMAO-stimulated increase in aortic TF and VCAM1. C57/BL6 mice were put on a choline diet with and without FMC in the drinking water. (*A*) Aortic tissue was subjected to immunohistochemistry using antibodies against TF, VCAM1, and the endothelial marker CD31. (*B*) Mean OD was quantified from three different anatomical sides and three data points are plotted for each animal. (*B*, lower panel) Levels of plasma TMAO, TMA, and choline were quantified via LC/MS/MS and (*C*) correlated with endothelial TF and VCAM1 expression. Results are presented as mean±SEM. Pairwise comparison was performed using a Mann–Whitney test. Correlation of TMA and TMAO levels with TF or VCAM1 mean endothelial OD was performed using non-parametric Spearman correlation.

phenotypes associated with heightened TMAO levels (e.g. platelet reactivity and thrombosis potential) has not yet been explored. It is notable that a recent study investigated the role of PERK inhibition in vascular intimal hyperplasia and restenosis.[89] The PERK inhibitor SK2606414 was reported to reduce tumour necrosis factor (TNF) α-induced TF expression in cultured rat aortic rings, and oral administration of SK2606414 to C57BL/6 mice prevented occlusive thrombosis in a $FeCl_3$ arterial injury model.[89] However, in that study, neither the involvement of TMAO, or TF, in the anti-thrombotic properties of the PERK inhibitor were explored. It should also be noted that beyond PERK, there are numerous alternative candidate pathways through which TMAO may affect TF expression. For example, TMAO has been shown to activate known

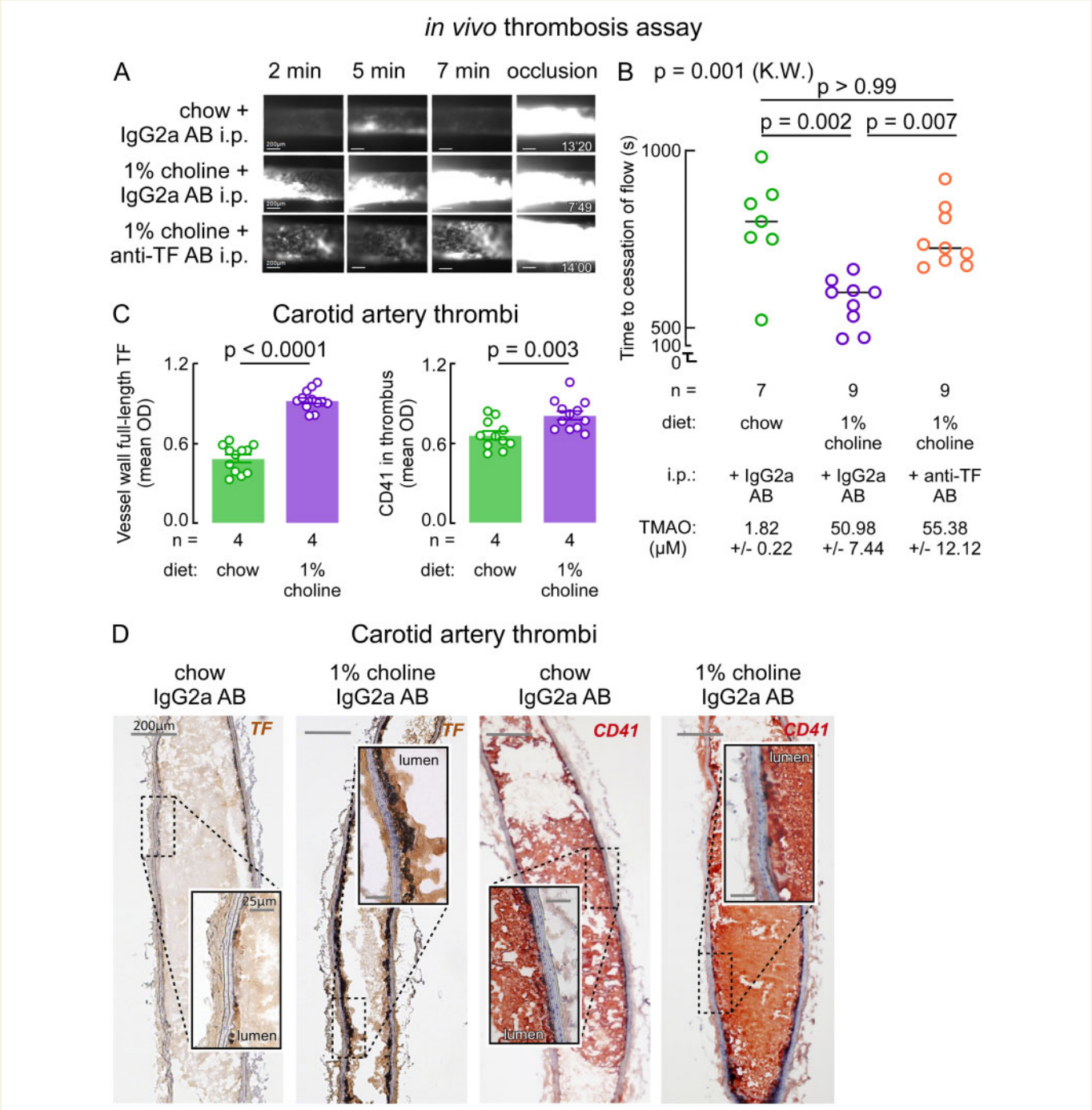

Figure 6 A TF-inhibitory antibody prevents the TMAO-associated enhancement in thrombus formation following arterial injury. C57/BL6 mice were put on a chow or choline diet for 10 days. The animals then received either an isotype control antibody (IgG2a) or the TF-inhibitory antibody (1H1) prior to a ferric chloride injury *in vivo* thrombosis model. (*A*) Intravital microscopy of rhodamine-labelled platelets during the *in vivo* thrombosis model was used to monitor thrombus formation in the animals on a chow diet with a control antibody, choline diet with a control antibody, and choline diet with a TF-neutralizing antibody and (*B*) time to cessation of flow assessed. Carotid thrombi of animals on chow or choline diet that received the control antibody were stained for TF and the platelet marker CD41 via immunohistochemistry. (*C*) Mean OD for vessel wall-associated thrombus TF and thrombus CD41 of three different sides (three data points for each animal are plotted) quantified by an imaging software. (*D*) Representative Immunohistochemistry images. Results are presented as mean±SEM. Global *P*-values shown were obtained by non-parametric Kruskal–Wallis test with Dunn's multiple comparisons *post hoc* test to compare occlusion time. Differences between two groups were assessed using a Mann–Whitney test.

potential drivers of TF expression including NFκB dependent endothelial cell activation,[36,37] inflammasome activation and oxidative stress,[17,85,90,91] as well as mitogen-activated protein kinase signalling and TNFα release[36,92]—all of which have been shown to induce TF expression in the vasculature.[41,42,47,93] Moreover, TF facilitates adverse signalling via protease-activated receptors through FXa and thrombin

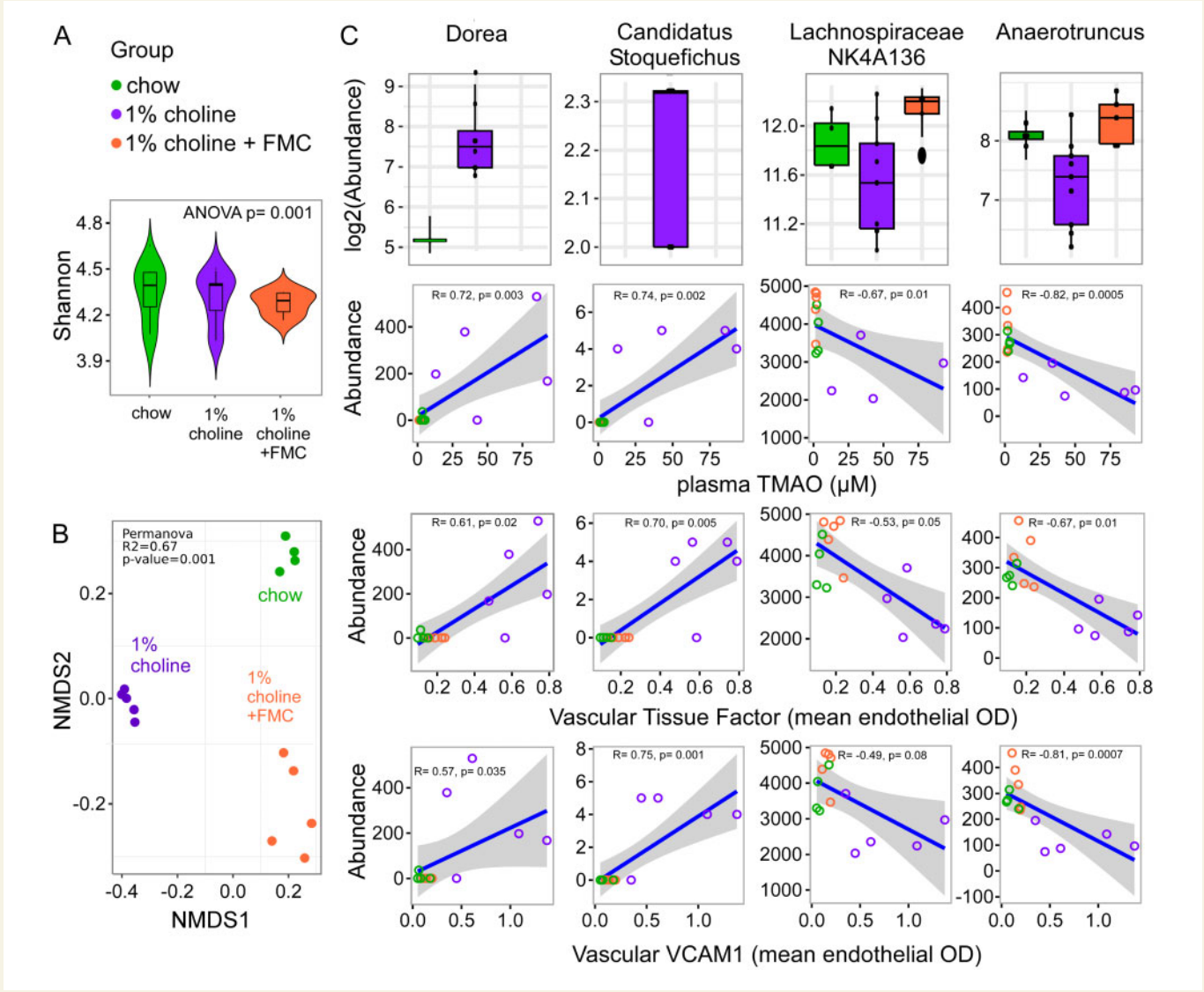

Figure 7 The gut microbiota choline TMA-lyase inhibitor FMC shifts the choline diet-induced changes in caecal microbial community associated with vascular TF and VCAM1. (*A*) Shannon diversity indices distinguishing chow, choline, and choline+FMC samples. Statistical analysis was performed using ANOVA. (*B*) NMDS based on Bray–Curtis index between the caecal microbiota recovered from mice that were on indicated diets. Statistical analysis was performed using permutational multivariate ANOVA with R^2 values for % variance explained by diet being the variable of interest. (*C*, upper panel) Statistically significant (Benjamini–Hochberg false discovery rate; $P < 0.05$) genera differentiating three groups (chow, choline, and choline+FMC). Plotted are interquartile ranges (IQRs) (boxes). The dark line in the box is the median, lower whiskers represent smallest observation (≥25% quantile—1.5×IQR), upper whiskers largest observation (≤75% quantile—1.5×IQR) with outliers as dots outside of the box. (*C*, second panel) Scatter plots based on linear regression showing correlation between abundance of indicated genera with plasma TMAO (μM) levels, (*C*, third panel) endothelial TF protein and (*C*, fourth panel) endothelial VCAM1 protein in mouse aortas on the indicated diets, expressed as OD within the annotated endothelial layer quantified by immunofluorescence (as described in Section 2). R^2 and *P*-values are indicated in each panel. For all panels, the same colour scheme was used for data to indicate animal diet: chow (green), choline (purple), and choline+FMC (red). The grey area shows the 95% CI.

generation.[94,95] Given the present findings that TMAO induces vascular endothelial cell TF expression *in vivo*, the role of TMAO in inducing TF-related pathologies merits further investigation.

Interestingly, we observed no impact of TMAO on TF expression in human monocytic cells while endothelial TF production was strongly increased. The contribution of TF originating from different cellular sources (vessel wall and blood cells) to thrombus generation in different disease models has been debated in the past. In addition to haematopoietic TF,[65] bone marrow transplantation studies coupled with microvascular and macrovascular thrombosis models, confirmed that vessel wall TF is a key contributor to arterial thrombosis formation *in vivo*.[50,51]

While our recent approaches towards the treatment of CVD have made tremendous advances, it is widely recognized that there still exists considerable residual clinical risk. Despite aggressive preventive efforts and the use of anti-platelet agents, atherothrombotic events are still the major cause of mortality. It is notable, however, that results from recent clinical trials show that this residual atherothrombotic event risk is in

part mitigated by targeting the extrinsic clotting pathway via FXa inhibitors.[96–98] However, use of FXa inhibitors and other treatment options for patients presenting with a pro-thrombotic state (i.e. chronic coronary syndromes) remain challenged by excess bleeding risks as an adverse complication.[99]

In previous studies, we showed that targeted inhibition of gut microbe-dependent TMAO production by provision of FMC served as a mechanism to inhibit thrombosis potential without adverse bleeding as a complication, since platelet hyper-responsiveness was reversed to normal.[22] Here, provision of FMC almost completely abolished TMAO-associated vascular endothelial cell TF and VCAM1 expression, while visual inspection of the adventitial compartment TF expression appears to remain intact. Collectively, the present and past studies suggest that modulation of the gut microbe—TMAO—TF axis (e.g. via dietary interventions, or targeted non-lethal small molecule inhibitors of microbial TMA generation) represents a novel avenue to selectively target pathological endothelial TF expression, extrinsic clotting cascade activation, and thrombosis, while preserving haemostasis. Translation of agents like FMC thus far only used in preclinical models to human interventions studies remains an attractive goal.

Supplementary material

Supplementary material is available at *Cardiovascular Research* online.

Authors' contributions

M.W. participated in the design of all studies, performed experiments and the statistical analysis, and drafted the manuscript. M.W. performed *ex vivo* mouse experiments. J.F. and A.H. assisted with immunofluorescence experiments; C.T. assisted with *in vitro* experiments, and J.A.B. helped with animal studies. X.S.L. and Z.W. assisted with mass spectrometry studies. F.M., L.R., C.M.M. and T.F.L. contributed clinical study samples and assisted with data analysis from the Swiss ACS cohort. N.S. assisted with microbe composition analyses, and L.L. helped with statistical analysis. J.A.D. and U.L. provided critical scientific input and discussions. S.L.H. and U.R. conceived, designed, and supervised all experiments and participated in the drafting and editing of the article. All authors contributed to the critical review of the manuscript.

Acknowledgements

We thank Dr Ajaykumar Zalavadia for his assistance in immunohistochemistry quantifications.

Conflict of interest: We have read the journal's policy and the authors of this manuscript have the following competing interests: Z.W. and S.L.H. report being named as co-inventor on pending and issued patents held by the Cleveland Clinic relating to cardiovascular diagnostics and therapeutics, and being eligible to receive royalty payments for inventions or discoveries related to cardiovascular diagnostics or therapeutics from Cleveland Heart Lab, a subsidiary of Quest Diagnostics, Zehna Therapeutics, and Procter & Gamble. S.L.H. also reports being a paid consultant for Zehna Therapeutics and Procter & Gamble, and having received research funds from Zehna Therapeutics, Procter & Gamble, and Roche Diagnostics. T.F.L. and C.M.M. were supported by grants from AstraZeneca, Roche Diagnostics, Medtronic, and Eli Lilly for the SPUM-ACS cohort. The other authors have reported that they have no relationships relevant to the contents of this article to disclose.

Funding

This work is supported by grants from the NIH and Office of Dietary Supplements (P01 HL147823, R01HL103866), and the Leducq Foundation. M.W. is supported by an award from the Deutsche Forschungsgemeinschaft (WI 5229/1-1). J.F. is participant in the BIH-Charité Clinician Scientist program funded by Charité–Universitätsmedizin and Berlin institute of health. The SPUM-ACS cohort was supported by the Swiss National Research Foundation and unrestricted grants from AstraZeneca, Roche Diagnostics, Medtronic, both Switzerland and Eli Lilly, Indianapolis, USA.

Data availability

There are restrictions to the availability of clinical data generated in this study as we do not have permission in our informed consent from research subjects to share data outside of our institution without their authorization.

Sequencing datasets used for community composition analysis were deposited in NCBI's Sequence Read Archive Database under BioProject # PRJNA689550. All other data are contained within the manuscript and/or Supplementary material online.

References

1. Aron-Wisnewsky J, Clément K. The gut microbiome, diet, and links to cardiometabolic and chronic disorders. *Nat Rev Nephrol* 2016;**12**:169–181.
2. Kasahara K, Rey FE. The emerging role of gut microbial metabolism on cardiovascular disease. *Curr Opin Microbiol* 2019;**50**:64–70.
3. Tang WHW, Bäckhed F, Landmesser U, Hazen SL. Intestinal microbiota in cardiovascular health and disease: JACC state-of-the-art review. *J Am Coll Cardiol* 2019;**73**:2089–2105.
4. Warmbrunn MV, Herrema H, Aron-Wisnewsky J, Soeters MR, Van Raalte DH, Nieuwdorp M. Gut microbiota: a promising target against cardiometabolic diseases. *Expert Rev Endocrinol Metab* 2020;**15**:13–27.
5. Witkowski M, Weeks TL, Hazen SL. Gut microbiota and cardiovascular disease. *Circ Res* 2020;**127**:553–570.
6. Koren O, Spor A, Felin J, Fåk F, Stombaugh J, Tremaroli V, Behre CJ, Knight R, Fagerberg B, Ley RE, Bäckhed F. Human oral, gut, and plaque microbiota in patients with atherosclerosis. *Proc Natl Acad Sci USA* 2011;**108(Suppl. 1)**:4592–4598.
7. Wang Z, Klipfell E, Bennett BJ, Koeth R, Levison BS, Dugar B, Feldstein AE, Britt EB, Fu X, Chung YM, Wu Y, Schauer P, Smith JD, Allayee H, Tang WH, DiDonato JA, Lusis AJ, Hazen SL. Gut flora metabolism of phosphatidylcholine promotes cardiovascular disease. *Nature* 2011;**472**:57–63.
8. Pluznick JL, Protzko RJ, Gevorgyan H, Peterlin Z, Sipos A, Han J, Brunet I, Wan LX, Rey F, Wang T, Firestein SJ, Yanagisawa M, Gordon JI, Eichmann A, Peti-Peterdi J, Caplan MJ. Olfactory receptor responding to gut microbiota-derived signals plays a role in renin secretion and blood pressure regulation. *Proc Natl Acad Sci USA* 2013;**110**:4410–4415.
9. Chen PB, Black AS, Sobel AL, Zhao Y, Mukherjee P, Molparia B, Moore NE, Aleman Muench GR, Wu J, Chen W, Pinto AFM, Maryanoff BE, Saghatelian A, Soroosh P, Torkamani A, Leman LJ, Ghadiri MR. Directed remodeling of the mouse gut microbiome inhibits the development of atherosclerosis. *Nat Biotechnol* 2020;**38**:1288–1297.
10. Nemet I, Saha PP, Gupta N, Zhu W, Romano KA, Skye SM, Cajka T, Mohan ML, Li L, Wu Y, Funabashi M, Ramer-Tait AE, Naga Prasad SV, Fiehn O, Rey FE, Tang WHW, Fischbach MA, DiDonato JA, Hazen SL. A cardiovascular disease-linked gut microbial metabolite acts via adrenergic receptors. *Cell* 2020;**180**:862–877.e822.
11. Koeth RA, Wang Z, Levison BS, Buffa JA, Org E, Sheehy BT, Britt EB, Fu X, Wu Y, Li L, Smith JD, DiDonato JA, Chen J, Li H, Wu GD, Lewis JD, Warrier M, Brown JM, Krauss RM, Tang WHW, Bushman FD, Lusis AJ, Hazen SL. Intestinal microbiota metabolism of L-carnitine, a nutrient in red meat, promotes atherosclerosis. *Nat Med* 2013;**19**:576–585.
12. Tang WH, Wang Z, Levison BS, Koeth RA, Britt EB, Fu X, Wu Y, Hazen SL. Intestinal microbial metabolism of phosphatidylcholine and cardiovascular risk. *N Engl J Med* 2013;**368**:1575–1584.
13. Miao J, Ling AV, Manthena PV, Gearing ME, Graham MJ, Crooke RM, Croce KJ, Esquejo RM, Clish CB, Vicent D, Biddinger SB, Morbid Obesity Study Group. Flavin-

containing monooxygenase 3 as a potential player in diabetes-associated atherosclerosis. *Nat Commun* 2015;**6**:6498.
14. Warrier M, Shih DM, Burrows AC, Ferguson D, Gromovsky AD, Brown AL, Marshall S, McDaniel A, Schugar RC, Wang Z, Sacks J, Rong X, Vallim TA, Chou J, Ivanova PT, Myers DS, Brown HA, Lee RG, Crooke RM, Graham MJ, Liu X, Parini P, Tontonoz P, Lusis AJ, Hazen SL, Temel RE, Brown JM. The TMAO-generating enzyme flavin monooxygenase 3 is a central regulator of cholesterol balance. *Cell Rep* 2015;**10**:326–338.
15. Stubbs JR, House JA, Ocque AJ, Zhang S, Johnson C, Kimber C, Schmidt K, Gupta A, Wetmore JB, Nolin TD, Spertus JA, Yu AS. Serum trimethylamine-N-oxide is elevated in CKD and correlates with coronary atherosclerosis burden. *JASN* 2016;**27**: 305–313.
16. Yazdekhasti N, Brandsch C, Schmidt N, Schloesser A, Huebbe P, Rimbach G, Stangl GI. Fish protein increases circulating levels of trimethylamine-N-oxide and accelerates aortic lesion formation in apoE null mice. *Mol Nutr Food Res* 2016;**60**: 358–368.
17. Boini KM, Hussain T, Li PL, Koka S. Trimethylamine-N-oxide instigates NLRP3 inflammasome activation and endothelial dysfunction. *Cell Physiol Biochem* 2017;**44**: 152–162.
18. Schugar RC, Shih DM, Warrier M, Helsley RN, Burrows A, Ferguson D, Brown AL, Gromovsky AD, Heine M, Chatterjee A, Li L, Li XS, Wang Z, Willard B, Meng Y, Kim H, Che N, Pan C, Lee RG, Crooke RM, Graham MJ, Morton RE, Langefeld CD, Das SK, Rudel LL, Zein N, McCullough AJ, Dasarathy S, Tang WHW, Erokwu BO, Flask CA, Laakso M, Civelek M, Naga Prasad SV, Heeren J, Lusis AJ, Hazen SL, Brown JM. The TMAO-producing enzyme flavin-containing monooxygenase 3 regulates obesity and the beiging of white adipose tissue. *Cell Rep* 2017;**20**:279.
19. Shih DM, Zhu W, Schugar RC, Meng Y, Jia X, Miikeda A, Wang Z, Zieger M, Lee R, Graham M, Allayee H, Cantor RM, Mueller C, Brown JM, Hazen SL, Lusis AJ. Genetic deficiency of flavin-containing monooxygenase 3 (Fmo3) protects against thrombosis but has only a minor effect on plasma lipid levels-brief report. *Arterioscler Thromb Vasc Biol* 2019;**39**:1045–1054.
20. Pathak P, Helsley RN, Brown AL, Buffa JA, Choucair I, Nemet I, Gogonea CB, Gogonea V, Wang Z, Garcia-Garcia JC, Cai L, Temel R, Sangwan N, Hazen SL, Brown JM. Small molecule inhibition of gut microbial choline trimethylamine lyase activity alters host cholesterol and bile acid metabolism. *Am J Physiol Heart Circ Physiol* 2020;**318**:H1474–H1486.
21. Zhang X, Li Y, Yang P, Liu X, Lu L, Chen Y, Zhong X, Li Z, Liu H, Ou C, Yan J, Chen M. Trimethylamine-N-oxide promotes vascular calcification through activation of NLRP3 (nucleotide-binding domain, leucine-rich-containing family, pyrin domain-containing-3) inflammasome and NF-κB (nuclear factor κB) signals. *Arterioscler Thromb Vasc Biol* 2020;**40**:751–765.
22. Zhu W, Gregory JC, Org E, Buffa JA, Gupta N, Wang Z, Li L, Fu X, Wu Y, Mehrabian M, Sartor RB, McIntyre TM, Silverstein RL, Tang WHW, DiDonato JA, Brown JM, Lusis AJ, Hazen SL. Gut microbial metabolite TMAO enhances platelet hyperreactivity and thrombosis risk. *Cell* 2016;**165**:111–124.
23. Haghikia A, Li XS, Liman TG, Bledau N, Schmidt D, Zimmermann F, Kränkel N, Widera C, Sonnenschein K, Haghikia A, Weissenborn K, Fraccarollo D, Heimesaat MM, Bauersachs J, Wang Z, Zhu W, Bavendiek U, Hazen SL, Endres M, Landmesser U. Gut microbiota-dependent trimethylamine N-oxide predicts risk of cardiovascular events in patients with stroke and is related to proinflammatory monocytes. *ATVB* 2018;**38**:2225–2235.
24. Zhu W, Buffa JA, Wang Z, Warrier M, Schugar R, Shih DM, Gupta N, Gregory JC, Org E, Fu X, Li L, DiDonato JA, Lusis AJ, Brown JM, Hazen SL. Flavin monooxygenase 3, the host hepatic enzyme in the metaorganismal trimethylamine N-oxide-generating pathway, modulates platelet responsiveness and thrombosis risk. *J Thromb Haemost* 2018;**16**:1857–1872.
25. Craciun S, Balskus EP. Microbial conversion of choline to trimethylamine requires a glycyl radical enzyme. *Proc Natl Acad Sci USA* 2012;**109**:21307–21312.
26. Cheung W, Keski-Rahkonen P, Assi N, Ferrari P, Freisling H, Rinaldi S, Slimani N, Zamora-Ros R, Rundle M, Frost G, Gibbons H, Carr E, Brennan L, Cross AJ, Pala V, Panico S, Sacerdote C, Palli D, Tumino R, Kühn T, Kaaks R, Boeing H, Floegel A, Mancini F, Boutron-Ruault MC, Baglietto L, Trichopoulou A, Naska A, Orfanos P, Scalbert A. A metabolomic study of biomarkers of meat and fish intake. *Am J Clin Nutr* 2017;**105**:600–608.
27. Lang DH, Yeung CK, Peter RM, Ibarra C, Gasser R, Itagaki K, Philpot RM, Rettie AE. Isoform specificity of trimethylamine N-oxygenation by human flavin-containing monooxygenase (FMO) and P450 enzymes: selective catalysis by FMO3. *Biochem Pharmacol* 1998;**56**:1005–1012.
28. Schiattarella GG, Sannino A, Toscano E, Giugliano G, Gargiulo G, Franzone A, Trimarco B, Esposito G, Perrino C. Gut microbe-generated metabolite trimethylamine-N-oxide as cardiovascular risk biomarker: a systematic review and dose-response meta-analysis. *Eur Heart J* 2017;**38**:2948–2956.
29. Guasti L, Galliazzo S, Molaro M, Visconti E, Pennella B, Gaudio GV, Lupi A, Grandi AM, Squizzato A. TMAO as a biomarker of cardiovascular events: a systematic review and meta-analysis. *Intern Emerg Med* 2021;**16**:201–207.
30. Farhangi MA, Vajdi M, Asghari-Jafarabadi M. Gut microbiota-associated metabolite trimethylamine N-Oxide and the risk of stroke: a systematic review and dose-response meta-analysis. *Nutr J* 2020;**19**:76.
31. Li W, Huang A, Zhu H, Liu X, Huang X, Huang Y, Cai X, Lu J, Huang Y. Gut microbiota-derived trimethylamine N-oxide is associated with poor prognosis in patients with heart failure. *Med J Aust* 2020;**213**:374–379.
32. Fu Q, Zhao M, Wang D, Hu H, Guo C, Chen W, Li Q, Zheng L, Chen B. Coronary plaque characterization assessed by optical coherence tomography and plasma trimethylamine-N-oxide levels in patients with coronary artery disease. *Am J Cardiol* 2016;**118**:1311–1315.
33. Liu X, Xie Z, Sun M, Wang X, Li J, Cui J, Zhang F, Yin L, Huang D, Hou J, Tian J, Yu B. Plasma trimethylamine N-oxide is associated with vulnerable plaque characteristics in CAD patients as assessed by optical coherence tomography. *Int J Cardiol* 2018;**265**: 18–23.
34. Tan Y, Sheng Z, Zhou P, Liu C, Zhao H, Song L, Li J, Zhou J, Chen Y, Wang L, Qian H, Sun Z, Qiao S, Xu B, Gao R, Yan H. Plasma trimethylamine N-oxide as a novel biomarker for plaque rupture in patients with ST-segment-elevation myocardial infarction. *Circ Cardiovasc Interv* 2019;**12**:e007281. [CVOCROSSCVO]
35. Koay YC, Chen YC, Wali JA, Luk AWS, Li M, Doma H, Reimark R, Zaldivia MTK, Habtom HT, Franks AE, Fusco-Allison G, Yang J, Holmes A, Simpson SJ, Peter K, O'Sullivan JF. Plasma levels of trimethylamine-N-oxide can be increased with 'healthy' and 'unhealthy' diets and do not correlate with the extent of atherosclerosis but with plaque instability. *Cardiovasc Res* 2021;**117**:435–449.
36. Seldin MM, Meng Y, Qi H, Zhu W, Wang Z, Hazen SL, Lusis AJ, Shih DM. Trimethylamine N-oxide promotes vascular inflammation through signaling of mitogen-activated protein kinase and nuclear factor-κB. *J Am Heart Assoc* 2016;**5**: e002767.
37. Ma G, Pan B, Chen Y, Guo C, Zhao M, Zheng L, Chen B. Trimethylamine N-oxide in atherogenesis: impairing endothelial self-repair capacity and enhancing monocyte adhesion. *Biosci Rep* 2017;**37**:BSR20160244. [CVOCROSSCVO]
38. Zhu W, Wang Z, Tang WHW, Hazen SL. Gut microbe-generated trimethylamine N-oxide from dietary choline is prothrombotic in subjects. *Circulation* 2017;**135**: 1671–1673.
39. Roberts AB, Gu X, Buffa JA, Hurd AG, Wang Z, Zhu W, Gupta N, Skye SM, Cody DB, Levison BS, Barrington WT, Russell MW, Reed JM, Duzan A, Lang JM, Fu X, Li L, Myers AJ, Rachakonda S, DiDonato JA, Brown JM, Gogonea V, Lusis AJ, Garcia-Garcia JC, Hazen SL. Development of a gut microbe-targeted nonlethal therapeutic to inhibit thrombosis potential. *Nat Med* 2018;**24**:1407–1417.
40. Gong D, Zhang L, Zhang Y, Wang F, Zhao Z, Zhou X. Gut microbial metabolite trimethylamine N-oxide is related to thrombus formation in atrial fibrillation patients. *Am J Med Sci* 2019;**358**:422–428.
41. Witkowski M, Landmesser U, Rauch U. Tissue factor as a link between inflammation and coagulation. *Trends Cardiovasc Med* 2016;**26**:297–303.
42. Grover SP, Mackman N. Tissue factor in atherosclerosis and atherothrombosis. *Atherosclerosis* 2020;**307**:80–86.
43. Steffel J, Lüscher TF, Tanner FC. Tissue factor in cardiovascular diseases. *Circulation* 2006;**113**:722–731.
44. Witkowski M, Weithauser A, Tabaraie T, Steffens D, Krankel N, Witkowski M, Stratmann B, Tschoepe D, Landmesser U, Rauch-Kroehnert U. Micro-RNA-126 reduces the blood thrombogenicity in diabetes mellitus via targeting of tissue factor. *Arterioscler Thromb Vasc Biol* 2016;**36**:1263–1271.
45. Witkowski M, Tabaraie T, Steffens D, Friebel J, Dorner A, Skurk C, Witkowski M, Stratmann B, Tschoepe D, Landmesser U, Rauch U. MicroRNA-19a contributes to the epigenetic regulation of tissue factor in diabetes. *Cardiovasc Diabetol* 2018;**17**:34.
46. Witkowski M, Rauch U. Letter to the Editor: tissue factor of endothelial origin: Just another brick in the wall? *Trends Cardiovasc Med* 2017;**27**:155–156.
47. Szotowski B, Antoniak S, Poller W, Schultheiss H-P, Rauch U. Procoagulant soluble tissue factor is released from endothelial cells in response to inflammatory cytokines. *Circ Res* 2005;**96**:1233–1239.
48. Bogdanov VY, Balasubramanian V, Hathcock J, Vele O, Lieb M, Nemerson Y. Alternatively spliced human tissue factor: a circulating, soluble, thrombogenic protein. *Nat Med* 2003;**9**:458–462.
49. Toschi V, Gallo R, Lettino M, Fallon JT, Gertz SD, FernáNdez-Ortiz A, Chesebro JH, Badimon L, Nemerson Y, Fuster V, Badimon JJ. Tissue factor modulates the thrombogenicity of human atherosclerotic plaques. *Circulation* 1997;**95**:594–599.
50. Day SM, Reeve JL, Pedersen B, Farris DM, Myers DD, Im M, Wakefield TW, Mackman N, Fay WP. Macrovascular thrombosis is driven by tissue factor derived primarily from the blood vessel wall. *Blood* 2005;**105**:192–198.
51. Chou J, Mackman N, Merrill-Skoloff G, Pedersen B, Furie BC, Furie B. Hematopoietic cell-derived microparticle tissue factor contributes to fibrin formation during thrombus propagation. *Blood* 2004;**104**:3190–3197.
52. Klingenberg R, Heg D, Räber L, Carballo D, Nanchen D, Gencer B, Auer R, Jaguszewski M, Stähli BE, Jakob P, Templin C, Stefanini GG, Meier B, Vogt P, Roffi M, Maier W, Landmesser U, Rodondi N, Mach F, Windecker S, Jüni P, Lüscher TF, Matter CM. Safety profile of prasugrel and clopidogrel in patients with acute coronary syndromes in Switzerland. *Heart* 2015;**101**:854–863.
53. Li XS, Obeid S, Klingenberg R, Gencer B, Mach F, Räber L, Windecker S, Rodondi N, Nanchen D, Muller O, Miranda MX, Matter CM, Wu Y, Li L, Wang Z, Alamri HS, Gogonea V, Chung Y-M, Tang WHW, Hazen SL, Lüscher TF. Gut microbiota-dependent trimethylamine N-oxide in acute coronary syndromes: a prognostic marker for incident cardiovascular events beyond traditional risk factors. *Eur Heart J* 2017;**38**:814–824. [CVOCROSSCVO]

54. Wang Z, Levison BS, Hazen JE, Donahue L, Li XM, Hazen SL. Measurement of trimethylamine-N-oxide by stable isotope dilution liquid chromatography tandem mass spectrometry. *Anal Biochem* 2014;**455**:35–40.
55. Kirchhofer D, Moran P, Bullens S, Peale F, Bunting S. A monoclonal antibody that inhibits mouse tissue factor function. *J Thromb Haemost* 2005;**3**:1098–1099.
56. Shashar M, Belghasem ME, Matsuura S, Walker J, Richards S, Alousi F, Rijal K, Kolachalama VB, Balcells M, Odagi M, Nagasawa K, Henderson JM, Gautam A, Rushmore R, Francis J, Kirchhofer D, Kolandaivelu K, Sherr DH, Edelman ER, Ravid K, Chitalia VC. Targeting STUB1-tissue factor axis normalizes hyperthrombotic uremic phenotype without increasing bleeding risk. *Science Translational Medicine* 2017;**9**: eaam8475.
57. Szotowski B, Goldin-Lang P, Antoniak S, Bogdanov VY, Pathirana D, Pauschinger M, Dörner A, Kuehl U, Coupland S, Nemerson Y, Hummel M, Poller W, Hetzer R, Schultheiss HP, Rauch U. Alterations in myocardial tissue factor expression and cellular localization in dilated cardiomyopathy. *J Am Coll Cardiol* 2005;**45**: 1081–1089.
58. Bankhead P, Loughrey MB, Fernández JA, Dombrowski Y, McArt DG, Dunne PD, McQuaid S, Gray RT, Murray LJ, Coleman HG, James JA, Salto-Tellez M, Hamilton PW. QuPath: open source software for digital pathology image analysis. *Sci Rep* 2017; **7**:16878.
59. Consortium THMP. Structure, function and diversity of the healthy human microbiome. *Nature* 2012;**486**:207–214. [CVOCROSSCVO]
60. Caporaso JG, Kuczynski J, Stombaugh J, Bittinger K, Bushman FD, Costello EK, Fierer N, Peña AG, Goodrich JK, Gordon JI, Huttley GA, Kelley ST, Knights D, Koenig JE, Ley RE, Lozupone CA, McDonald D, Muegge BD, Pirrung M, Reeder J, Sevinsky JR, Turnbaugh PJ, Walters WA, Widmann J, Yatsunenko T, Zaneveld J, Knight R. QIIME allows analysis of high-throughput community sequencing data. *Nat Methods* 2010;**7**: 335–336.
61. Callahan BJ, McMurdie PJ, Rosen MJ, Han AW, Johnson AJ, Holmes SP. DADA2: high-resolution sample inference from Illumina amplicon data. *Nat Methods* 2016;**13**: 581–583.
62. McMurdie PJ, Holmes S. phyloseq: an R package for reproducible interactive analysis and graphics of microbiome census data. *PLoS One* 2013;**8**:e61217.
63. McMurdie PJ, Holmes S. Waste not, want not: why rarefying microbiome data is inadmissible. *PLoS Comput Biol* 2014;**10**:e1003531.
64. Benjamini Y. Discovering the false discovery rate. *J R Stat Soc Series B Stat Methodol* 2010;**72**:405–416.
65. Pawlinski R, Wang JG, Owens AP III, Williams J, Antoniak S, Tencati M, Luther T, Rowley JW, Low EN, Weyrich AS, Mackman N. Hematopoietic and nonhematopoietic cell tissue factor activates the coagulation cascade in endotoxemic mice. *Blood* 2010;**116**:806–814.
66. Witkowski M, Witkowski M, Saffarzadeh M, Friebel J, Tabaraie T, Ta Bao L, Chakraborty A, Dörner A, Stratmann B, Tschoepe D, Winter SJ, Krueger A, Ruf W, Landmesser U, Rauch U. Vascular miR-181b controls tissue factor-dependent thrombogenicity and inflammation in type 2 diabetes. *Cardiovasc Diabetol* 2020;**19**:20.
67. Witkowski M, Friebel J, Tabaraie T, Grabitz S, Dörner A, Taghipour L, Jakobs K, Stratmann B, Tschoepe D, Landmesser U, Rauch U. Metformin is associated with reduced tissue factor procoagulant activity in patients with poorly controlled diabetes. *Cardiovasc Drugs Ther* 2021;**35**:809–813.
68. Sambola A, Osende J, Hathcock J, Degen M, Nemerson Y, Fuster V, Crandall J, Badimon JJ. Role of risk factors in the modulation of tissue factor activity and blood thrombogenicity. *Circulation* 2003;**107**:973–977.
69. Moons AHM, Levi M, Peters RJG. Tissue factor and coronary artery disease. *Cardiovasc Res* 2002;**53**:313–325.
70. Suefuji H, Ogawa H, Yasue H, Kaikita K, Soejima H, Motoyama T, Mizuno Y, Oshima S, Saito T, Tsuji I, Kumeda K, Kamikubo Y, Nakamura S. Increased plasma tissue factor levels in acute myocardial infarction. *Am Heart J* 1997;**134**:253–259.
71. Palmerini T, Tomasi L, Barozzi C, Della Riva D, Mariani A, Taglieri N, Leone O, Ceccarelli C, Branzi A, Ahamed J. Detection of tissue factor antigen and coagulation activity in coronary artery thrombi isolated from patients with ST-segment elevation acute myocardial infarction. *Eur Heart J* 2013;**34**:P1275.
72. Iacoviello L, Di Castelnuovo A, de Curtis A, Agnoli C, Frasca G, Mattiello A, Matullo G, Ricceri F, Sacerdote C, Grioni S, Tumino R, Napoleone E, Lorenzet R, de Gaetano G, Panico S, Donati Maria B. Circulating tissue factor levels and risk of stroke. *Stroke* 2015;**46**:1501–1507.
73. Tang WHW, Wang Z, Li XS, Fan Y, Li DS, Wu Y, Hazen SL. Increased trimethylamine N-oxide portends high mortality risk independent of glycemic control in patients with type 2 diabetes mellitus. *Clin Chem* 2017;**63**:297–306.
74. Li XS, Obeid S, Wang Z, Hazen BJ, Li L, Wu Y, Hurd AG, Gu X, Pratt A, Levison BS, Chung Y-M, Nissen SE, Tang WHW, Mach F, Räber L, Nanchen D, Matter CM, Lüscher TF, Hazen SL. Trimethyllysine, a trimethylamine N-oxide precursor, provides near- and long-term prognostic value in patients presenting with acute coronary syndromes. *Eur Heart J* 2019;**40**:2700–2709.
75. Waleed KB, Tse G, Lu YK, Peng CN, Tu H, Ding LG, Xia YL, Wu SL, Li XT, Zhou HQ, Chen QY, Sun AM, Altaf A, Chang JL, Wang LL. Trimethylamine N-oxide is associated with coronary atherosclerotic burden in non-ST-segment myocardial infarction patients: SZ-NSTEMI prospective cohort study. *Rev Cardiovasc Med* 2021; **22**:231–238.
76. Sheng Z, Tan Y, Liu C, Zhou P, Li J, Zhou J, Chen R, Chen Y, Song L, Zhao H, Yan H. Relation of circulating trimethylamine N-oxide with coronary atherosclerotic burden in patients with ST-segment elevation myocardial infarction. *Am J Cardiol* 2019;**123**: 894–898.
77. Senthong V, Li XS, Hudec T, Coughlin J, Wu Y, Levison B, Wang Z, Hazen SL, Tang WH. Plasma trimethylamine N-oxide, a gut microbe-generated phosphatidylcholine metabolite, is associated with atherosclerotic burden. *J Am Coll Cardiol* 2016;**67**: 2620–2628.
78. Ma R, Fu W, Zhang J, Hu X, Yang J, Jiang H. TMAO: a potential mediator of clopidogrel resistance. *Sci Rep* 2021;**11**:6580.
79. Badimon L, Padró T, Vilahur G. Atherosclerosis, platelets and thrombosis in acute ischaemic heart disease. *Eur Heart J Acute Cardiovasc Care* 2012;**1**:60–74.
80. Badimon JJ, Lettino M, Toschi V, Fuster V, Berrozpe M, Chesebro JH, Badimon L. Local inhibition of tissue factor reduces the thrombogenicity of disrupted human atherosclerotic plaques: effects of tissue factor pathway inhibitor on plaque thrombogenicity under flow conditions. *Circulation* 1999;**99**:1780–1787.
81. Sun X, Jiao X, Ma Y, Liu Y, Zhang L, He Y, Chen Y. Trimethylamine N-oxide induces inflammation and endothelial dysfunction in human umbilical vein endothelial cells via activating ROS-TXNIP-NLRP3 inflammasome. *Biochem Biophys Res Commun* 2016; **481**:63–70.
82. Ke Y, Li D, Zhao M, Liu C, Liu J, Zeng A, Shi X, Cheng S, Pan B, Zheng L, Hong H. Gut flora-dependent metabolite Trimethylamine-N-oxide accelerates endothelial cell senescence and vascular aging through oxidative stress. *Free Radic Biol Med* 2018;**116**:88–100.
83. Singh GB, Zhang Y, Boini KM, Koka S. High mobility group box 1 mediates TMAO-induced endothelial dysfunction. *Int J Mol Sci* 2019;**20**:3570. [CVOCROSSCVO]
84. Yang G, Lin CC, Yang Y, Yuan L, Wang P, Wen X, Pan MH, Zhao H, Ho CT, Li S. Nobiletin prevents trimethylamine oxide-induced vascular inflammation via inhibition of the NF-κB/MAPK pathways. *J Agric Food Chem* 2019;**67**:6169–6176.
85. Chen M-L, Zhu X-H, Ran L, Lang H-D, Yi L, Mi M-T. Trimethylamine-N-oxide induces vascular inflammation by activating the NLRP3 inflammasome through the SIRT3-SOD2-mtROS signaling pathway. *J Am Heart Assoc* 2017;**6**:e006347.
86. Subramaniam S, Boukhlouf S, Fletcher C. A bacterial metabolite, trimethylamine N-oxide, disrupts the hemostasis balance in human primary endothelial cells but no coagulopathy in mice. *Blood Coagul Fibrinolysis* 2019;**30**:324–330.
87. Cheng X, Qiu X, Liu Y, Yuan C, Yang X. Trimethylamine N-oxide promotes tissue factor expression and activity in vascular endothelial cells: a new link between trimethylamine N-oxide and atherosclerotic thrombosis. *Thromb Res* 2019;**177**:110–116.
88. Chen S, Henderson A, Petriello MC, Romano KA, Gearing M, Miao J, Schell M, Sandoval-Espinola WJ, Tao J, Sha B, Graham M, Crooke R, Kleinridders A, Balskus EP, Rey FE, Morris AJ, Biddinger SB. Trimethylamine N-oxide binds and activates PERK to promote metabolic dysfunction. *Cell Metab* 2019;**30**:1141–1151.e1145.
89. Wang B, Zhang M, Urabe G, Huang Y, Chen G, Wheeler D, Dornbos DJ III, Huttinger A, Nimjee SM, Gong S, Guo L-W, Kent KC. PERK inhibition mitigates restenosis and thrombosis: a potential low-thrombogenic antirestenotic paradigm. *JACC Basic Transl Sci* 2020;**5**:245–263.
90. Li T, Chen Y, Gua C, Li X. Elevated circulating trimethylamine N-oxide levels contribute to endothelial dysfunction in aged rats through vascular inflammation and oxidative stress. *Front Physiol* 2017;**8**:350–350.
91. Brunt VE, Gioscia-Ryan RA, Casso AG, VanDongen NS, Ziemba BP, Sapinsley ZJ, Richey JJ, Zigler MC, Neilson AP, Davy KP, Seals DR. Trimethylamine-N-oxide promotes age-related vascular oxidative stress and endothelial dysfunction in mice and healthy humans. *Hypertension* 2020;**76**:101–112.
92. Geng J, Yang C, Wang B, Zhang X, Hu T, Gu Y, Li J. Trimethylamine N-oxide promotes atherosclerosis via CD36-dependent MAPK/JNK pathway. *Biomed Pharmacother* 2018;**97**:941–947.
93. Gaul DS, Weber J, van Tits LJ, Sluka S, Pasterk L, Reiner MF, Calatayud N, Lohmann C, Klingenberg R, Pahla J, Vdovenko D, Tanner FC, Camici GG, Eriksson U, Auwerx J, Mach F, Windecker S, Rodondi N, Lüscher TF, Winnik S, Matter CM. Loss of Sirt3 accelerates arterial thrombosis by increasing formation of neutrophil extracellular traps and plasma tissue factor activity. *Cardiovasc Res* 2018;**114**:1178–1188.
94. Friebel J, Weithauser A, Witkowski M, Rauch BH, Savvatis K, Dörner A, Tabaraie T, Kasner M, Moos V, Bösel D, Gotthardt M, Radke MH, Wegner M, Bobbert P, Lassner D, Tschöpe C, Schutheiss H-P, Felix SB, Landmesser U, Rauch U. Protease-activated receptor 2 deficiency mediates cardiac fibrosis and diastolic dysfunction. *Eur Heart J* 2019;**40**:3318–3332.
95. Weithauser A, Witkowski M, Rauch U. The role of protease-activated receptors for the development of myocarditis: possible therapeutic implications. *Curr Pharm Des* 2016;**22**:472–484.
96. Mega JL, Braunwald E, Wiviott SD, Bassand JP, Bhatt DL, Bode C, Burton P, Cohen M, Cook-Bruns N, Fox KA, Goto S, Murphy SA, Plotnikov AN, Schneider D, Sun X, Verheugt FW, Gibson CM. Rivaroxaban in patients with a recent acute coronary syndrome. *N Engl J Med* 2012;**366**:9–19.
97. Eikelboom JW, Connolly SJ, Bosch J, Dagenais GR, Hart RG, Shestakovska O, Diaz R, Alings M, Lonn EM, Anand SS, Widimsky P, Hori M, Avezum A, Piegas LS, Branch

KRH, Probstfield J, Bhatt DL, Zhu J, Liang Y, Maggioni AP, Lopez-Jaramillo P, O'Donnell M, Kakkar AK, Fox KAA, Parkhomenko AN, Ertl G, Störk S, Keltai M, Ryden L, Pogosova N, Dans AL, Lanas F, Commerford PJ, Torp-Pedersen C, Guzik TJ, Verhamme PB, Vinereanu D, Kim J-H, Tonkin AM, Lewis BS, Felix C, Yusoff K, Steg PG, Metsarinne KP, Cook Bruns N, Misselwitz F, Chen E, Leong D, Yusuf S. Rivaroxaban with or without aspirin in stable cardiovascular disease. *N Engl J Med* 2017;**377**:1319–1330.

98. Bonaca MP, Bauersachs RM, Anand SS, Debus ES, Nehler MR, Patel MR, Fanelli F, Capell WH, Diao L, Jaeger N, Hess CN, Pap AF, Kittelson JM, Gudz I, Mátyás L, Krievins DK, Diaz R, Brodmann M, Muehlhofer E, Haskell LP, Berkowitz SD, Hiatt WR. Rivaroxaban in peripheral artery disease after revascularization. *N Engl J Med* 2020;**382**:1994–2004.
99. Knuuti J, Wijns W, Saraste A, Capodanno D, Barbato E, Funck-Brentano C, Prescott E, Storey RF, Deaton C, Cuisset T, Agewall S, Dickstein K, Edvardsen T, Escaned J, Gersh BJ, Svitil P, Gilard M, Hasdai D, Hatala R, Mahfoud F, Masip J, Muneretto C, Valgimigli M, Achenbach S, Bax JJ, ESC Scientific Document Group. 2019 ESC Guidelines for the diagnosis and management of chronic coronary syndromes. *Eur Heart J* 2020;**41**:407–477.

Translational Perspective

The pro-thrombotic effects of the gut microbial TMAO pathway are shown to extend beyond enhancement of platelet responsiveness and include heightened vascular Tissue Factor (TF). In clinical studies, TMAO is shown to predict event risk in patients in the presence of anti-platelet drugs. In animal studies, TMAO elevation is shown to promote vascular endothelial TF expression and a TF-dependent pro-thrombotic effect. Pharmacological targeting of gut microbial choline TMA-lyase reduced host TMAO, vascular TF and abrogated the pro-thrombotic TMAO-associated phenotype. These studies suggest inhibiting the TMAO pathway may be a rational target for reducing residual risk in patients on anti-platelet therapy.